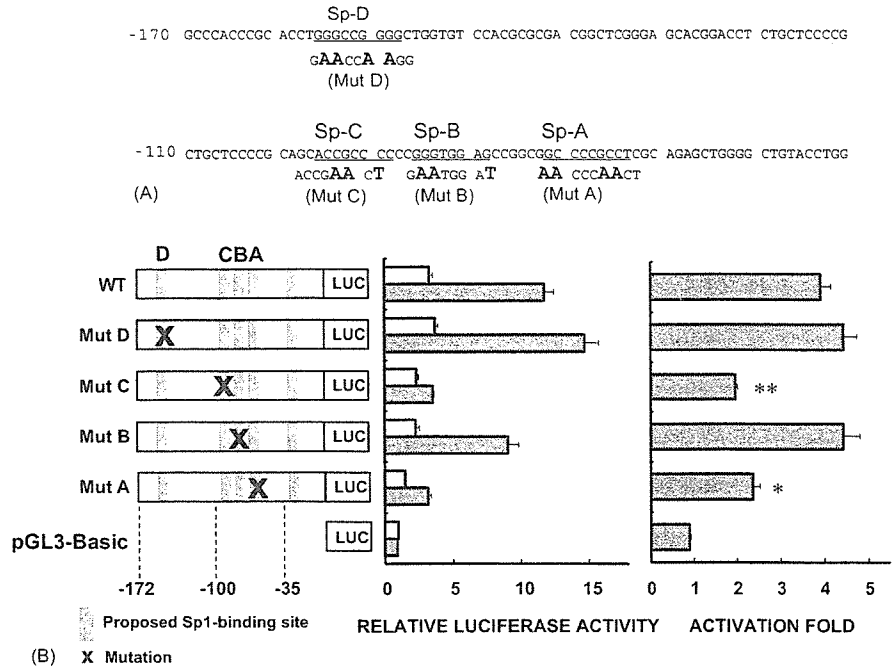

Fig. 3 – Mutational analysis of Sp1-binding sites in the Cdx2-responsive region in the PEPT1 promoter. (A) The nucleotide sequence of the promoter region from −170 to −41 is shown with the putative Sp1-binding elements (Sp-A, Sp-B, Sp-C, Sp-D, underlined). Site-directed mutations that destroy Sp1-binding elements were introduced individually and designated mut A, mut B, mut C and mut D. The nucleotides altered for mutational analysis are shown in bold letters under the wild-type sequence. (B) The mutated −172/+60 constructs (500 ng) and 500 ng of the Cdx2 expression vector or empty vector were transiently expressed in Caco-2 cells for luciferase assays. Firefly luciferase activity was normalized to *Renilla* luciferase activity. Data are reported as the relative fold-increase compared with the pGL3-Basic vector and as the ratio of Cdx2-expressing vector to empty vector, and represent the mean ± S.E. ($n = 3$). (* and **) Significantly different from wild type (WT), $^{*}p < 0.05$, $^{**}p < 0.01$.

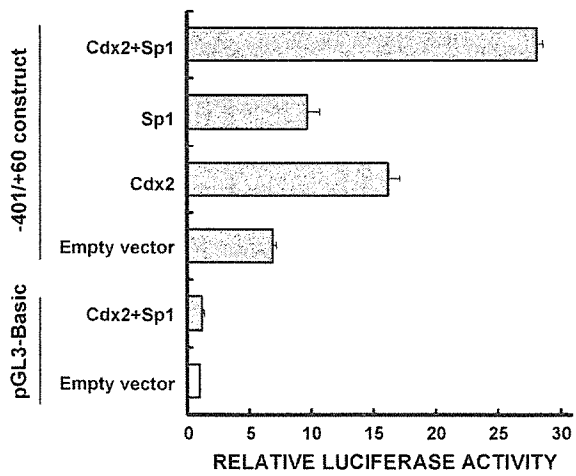

Fig. 4 – Synergistic activation of the PEPT1 promoter by Cdx2 and Sp1. Caco-2 cells were transiently transfected with 150 ng of the −401/+60 construct and the expression vector for Cdx2 (500 ng) or Sp1 (1000 ng). The total amount of transfected DNA (1650 ng) was kept constant by adding empty vectors. Data are reported as the relative fold-increase compared with pGL3-Basic and represent the mean ± S.E. ($n = 3$).

alternative methodology, the ChIP assay, to investigate the association of Cdx2 with the PEPT1 promoter. An approximately 200-bp fragment of the PEPT1 promoter covering the Cdx2-responsive region, which had the Sp1-binding sites, was recovered by immunoprecipitation of FLAG-Cdx2 from the transfected cells, whereas only a trace amount of the fragment was recovered from the mock-transfected cells (Fig. 6).

3.6. *The level of PEPT1 mRNA is correlated with that of CDX2 in the gastric samples with the intestinal metaplasia*

mRNA levels of PEPT1 and CDX2 in the human gastric samples, some with intestinal metaplasia, were determined using quantitative real-time PCR (Fig. 7). PEPT1 and CDX2 mRNA levels differed by more than 100-fold between the samples. The mRNA level of PEPT1 was highly correlated with that of CDX2. Furthermore, both PEPT1 and CDX2 were expressed at apparently higher levels in the samples diagnosed pathologically with intestinal metaplasia as compared to the normal tissue.

4. Discussion

The molecular mechanisms responsible for the intestine-specific expression of PEPT1 are largely unknown. In the

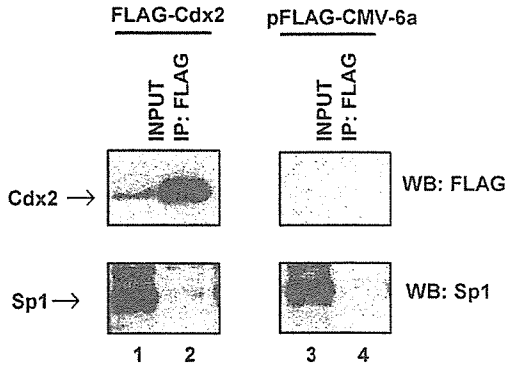

Fig. 5 – Physical interaction of Cdx2 with Sp1 protein. Whole-cell extracts of Caco-2 cells transfected with FLAG-Cdx2 or pFLAG-CMV-6a (empty vector) were subjected to immunoprecipitation followed by Western blotting. Proteins were immunoprecipitated with anti-FLAG M2 affinity gel (lanes 2 and 4, indicated as IP:FLAG). Whole-cell extracts before immunoprecipitation were also analyzed (lanes 1 and 3, indicated as INPUT). FLAG-Cdx2 and Sp1 protein were detected with anti-FLAG M2 monoclonal antibody (upper panels) and anti-Sp1 polyclonal antibody (lower panels), respectively.

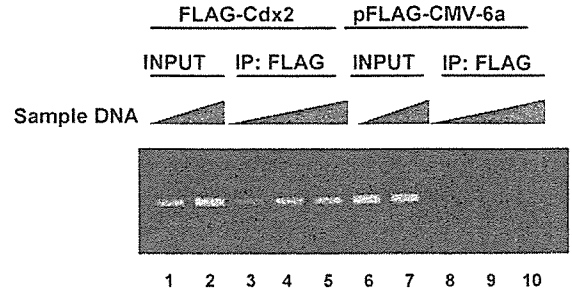

Fig. 6 – Association of Cdx2 with the PEPT1 promoter. Chromatin immunoprecipitation analysis of the endogenous PEPT1 promoter in Caco-2 cells transfected with FLAG-Cdx2 or pFLAG-CMV-6a (empty vector) was performed. The immunoprecipitated DNA fragments were purified and amplified by PCR with primers spanning the Cdx2-responsive region, and subjected to agarose gel electrophoresis. Serially diluted samples of DNA were used for PCR amplification. Lanes 1, 2 and 6, 7 indicate INPUT DNA. Lanes 3–5 and 8–10 show immunoprecipitated DNA.

present study, we provide the first evidence that Cdx2 regulates the transcription of PEPT1 using Caco-2 cells. Unlike other intestinal genes, such as the genes for LPH [10], claudin-2 [11] and UGTs [12], neither HNF-1α nor HNF-1β could trans-activate the PEPT1 promoter, although Cdx2 markedly enhanced the activity of the PEPT1 promoter. Deletion analysis revealed that the Cdx2-responsive region was located between bases −172 and −35 relative to the transcription start site. Computational analysis showed the lack of a canonical Cdx2-binding site in this region, but the presence of several GC-boxes which we previously identified as Sp1-binding sites. Sp1 has been reported to interact with various transcription factors or co-factors, such as estrogen receptor [17], p300/CREB-binding protein [18] and homeobox protein, Hox proteins [19]. Thus we tried to elucidate whether Cdx2 interacts with Sp1 to regulate the PEPT1 promoter.

Introducing mutations into Sp1-binding sites reduced the effect of Cdx2. Furthermore, co-expression of Cdx2 and Sp1 synergistically activated the PEPT promoter. These results suggest that the trans-activating effect of Cdx2 might be mediated via a Sp1-dependent mechanism. Among Sp1-binding sites located in Cdx2-responsive region, Sp-A, Sp-B and Sp-C were involved in the basal promoter activity, whereas only Sp-A and Sp-C appeared to be critical for Cdx2 effect, indicating that the regulatory effect of Cdx2 is site-dependent.

Co-immunoprecipitation of FLAG-tagged Cdx2 precipitated the endogenous Sp1 protein, suggesting the formation of a transcriptional complex involving Cdx2 and Sp1. In addition, ChIP assays indicated that Cdx2 protein was present on the

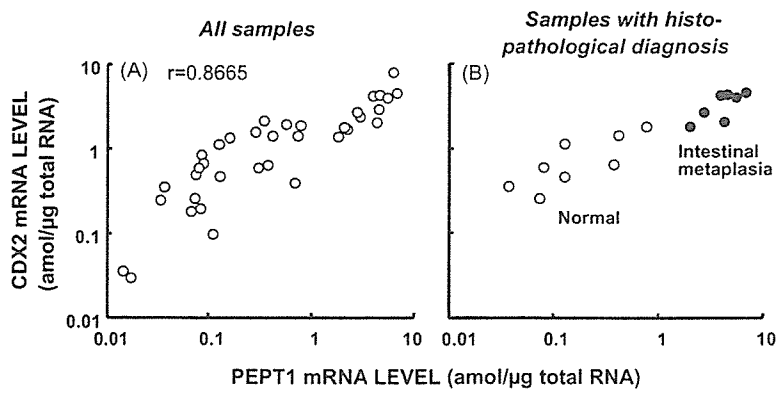

Fig. 7 – Correlation between PEPT1 and CDX2 mRNA levels in the human gastric tissue samples. The mRNA levels of PEPT1 and CDX2 were quantified with real-time PCR analysis in the gastric mucosal samples. Some of these tissue samples were diagnosed by a pathologist and proved to be intestinal metaplasia. (A) All samples were plotted. (B) The samples of patients diagnosed by a pathologist were plotted. Open and closed symbols indicate the normal samples and the samples proved to be intestinal metaplasia, respectively.

PEPT1 promoter at the whole cell level. Considering the lack of Cdx2-binding site in the Cdx2-responsive region and the functional and physical interaction between Cdx2 and Sp1 mentioned above, one explanation for the regulatory mechanism of Cdx2 may be that Cdx2 protein associates with the PEPT1 promoter via the complex formation with Sp1. Although Cdx2 has been reported to interact with the transcription factors such as HNF-1α [10–12] and GATA proteins [20], in all cases, Cdx2 directly binds to its cognate binding site on the promoter of target genes. By contrast, Cdx2 is speculated to exert its effect without direct binding to its cognate binding sequence on the PEPT1 promoter. The nature of the physical interaction between Cdx2 and Sp1 has yet to be determined. One possibility is that Cdx2 directly binds to Sp1 protein. Another possibility is indirect binding mediated by a common cofactor or some adaptor proteins. In both cases, to our knowledge, this is a novel mechanism of transcriptional regulation by Cdx2. Further studies will be needed to obtain the additional proof for supporting and fully characterizing this proposed mechanism.

In order to demonstrate the significance of Cdx2 for PEPT1 expression in vivo, we next investigated the expression profile of Cdx2 and PEPT1 mRNA using human tissue samples. In the gastric samples, some of which had intestinal metaplasia, PEPT1 and Cdx2 mRNA levels were highly correlated. The fact that ectopic expression of Cdx2 accompanied the expression of PEPT1 in human tissues strongly supports the role of Cdx2 demonstrated by in vitro reporter experiments. In addition, a recent study showed that expression of PEPT1 was induced in the gastric epithelium in a transgenic mouse expressing Cdx2 exclusively in the gastric epithelium [21].

The similarities between PEPT1 and Cdx2 in their expression profile are observed not only at the tissue level but also at the cellular level. PEPT1 is localized to brush-border membranes of the absorptive epithelial cells of the small intestine, and this protein is abundant at the tip of the villus and scarce at the crypt base [22]. Cdx2 also has a gradient of expression in the crypt–villus axis being primarily expressed in the villus [7].

It has been reported that intestinal PEPT1 is regulated by various factors [23], such as thyroid hormone [24], dietary conditions [25,26], diurnal rhythm [27] and a selective σ-ligand, pentazocine [28]. In addition, the ectopic induction of PEPT1 expression in the colon, where PEPT1 was not expressed under normal conditions, was observed in cases of functional deficiency of the small intestine such as ulcerative colitis, Crohn's disease and short-bowel syndrome [23]. It is not clear at present whether Cdx2 plays some parts in these regulatory functions. However, Cdx2 exerts physiological roles in the differentiation of intestinal epithelial cells and maintenance of intestinal phenotype. It is possible that Cdx2 helps to regulate colonic PEPT1 expression under such pathological conditions.

In conclusion, we demonstrated that Cdx2 regulated the PEPT1 promoter activity in Caco-2 cells using reporter assays, and confirmed the significance of Cdx2 in vivo in a correlation analysis of mRNA expression in human tissue samples. In addition, it may be possible that Cdx2 physically and functionally interacts with Sp1, and associates with the PEPT1 promoter although no cognate Cdx2-binding site is evident. These results collectively indicate that Cdx2 plays a key role in the transcriptional regulation for the intestine-specific expression of PEPT1, and have implications as a basis for future investigations of efficient enteral nutrition and drug therapy.

Acknowledgments

We are grateful to Dr. Eun Ran Suh (University of Pennsylvania) and Dr. Robert Tjian (University of California, Berkeley) for the generous gift of Cdx2 and Sp1 expression vectors, respectively. We also thank Dr. Marco Pontoglio (Institute Pasteur, Paris, France) for kindly providing Human HNF-1α and HNF-1β expression vectors.

This work was supported by the 21st Century COE Program "Knowledge Information Infrastructure for Genome Science", a Grant-in-Aid for Scientific Research from the Ministry of Education, Culture and Sports of Japan, and a Grant-in-Aid for Research on Advanced Medical Technology from the Ministry of Health, Labor and Welfare of Japan.

REFERENCES

[1] Daniel H. Molecular and integrative physiology of intestinal peptide transport. Annu Rev Physiol 2004;66:361–84.
[2] Terada T, Inui K. Peptide transporters: structure, function, regulation and application for drug delivery. Curr Drug Metabol 2004;5:85–94.
[3] Groneberg DA, Nickolaus M, Springer J, Doring F, Daniel H, Fischer A. Localization of the peptide transporter PEPT2 in the lung: implications for pulmonary oligopeptide uptake. Am J Pathol 2001;158:707–14.
[4] Berger UV, Hediger MA. Distribution of peptide transporter PEPT2 mRNA in the rat nervous system. Anat Embryol 1999;199:439–49.
[5] Groneberg DA, Doring F, Theis S, Nickolaus M, Fischer A, Daniel H. Peptide transport in the mammary gland: expression and distribution of PEPT2 mRNA and protein. Am J Physiol Endocrinol Metab 2002;282:E1172–9.
[6] Shimakura J, Terada T, Katsura T, Inui K. Characterization of the human peptide transporter PEPT1 promoter: Sp1 functions as a basal transcriptional regulator of human PEPT1. Am J Physiol Gastrointest Liver Physiol 2005;289:G471–7.
[7] Silberg DG, Swain GP, Suh ER, Traber PG. Cdx1 and Cdx2 expression during intestinal development. Gastroenterology 2000;119:961–71.
[8] Suh E, Traber PG. An intestine-specific homeobox gene regulates proliferation and differentiation. Mol Cell Biol 1996;16:619–25.
[9] Suh E, Chen L, Taylor J, Traber PG. A homeodomain protein related to caudal regulates intestine-specific gene transcription. Mol Cell Biol 1994;14:7340–51.
[10] Mitchelmore C, Troelsen JT, Spodsberg N, Sjostrom H, Noren O. Interaction between the homeodomain proteins Cdx2 and HNF1alpha mediates expression of the lactase-phlorizin hydrolase gene. Biochem J 2000;346:529–35.
[11] Sakaguchi T, Gu X, Golden HM, Suh E, Rhoads DB, Reinecker HC. Cloning of the human claudin-2 5′-flanking region revealed a TATA-less promoter with conserved binding sites in mouse and human for caudal-related homeodomain proteins and hepatocyte nuclear factor-1alpha. J Biol Chem 2002;277:21361–70.
[12] Gregory PA, Lewinsky RH, Gardner-Stephen DA, Mackenzie PI. Coordinate regulation of the human UDP

glucuronosyltransferase 1A8, 1A9, and 1A10 genes by hepatocyte nuclear factor 1α and the caudal-related homeodomain protein 2. Mol Pharmacol 2004;65:953–63.
[13] Almeida R, Silva E, Santos-Silva F, Silberg DG, Wang J, De Bolos C, et al. Expression of intestinespecific transcription factors, CDX1 and CDX2, in intestinal metaplasia and gastric carcinomas. J Pathol 2003;199:36–40.
[14] Terada T, Shimada Y, Pan X, Kishimoto K, Sakurai T, Doi R, et al. Expression profiles of various transporters for oligopeptides, amino acids and organic ions along the human digestive tract. Biochem Pharmacol 2005;70: 1756–63.
[15] Baumhueter S, Mendel DB, Conley PB, Kuo CJ, Turk C, Graves MK, et al. HNF-1 shares three sequence motifs with the POU domain proteins and is identical to LF-B1 and APF. Genes Dev 1990;4:372–9.
[16] Mendel DB, Crabtree GR. HNF-1, a member of a novel class of dimerizing homeodomain proteins. J Biol Chem 1991;266:677–80.
[17] Sun JM, Spencer VA, Li L, Yu Chen H, Yu J, Davie JR. Estrogen regulation of trefoil factor 1 expression by estrogen receptor α and Sp proteins. Exp Cell Res 2005;302:96–107.
[18] Jang SI, Steinert PM. Loricrin expression in cultured human keratinocytes is controlled by a complex interplay between transcription factors of the Sp1, CREB, AP1, and AP2 families. J Biol Chem 2002;277:42268–79.
[19] Suzuki M, Ueno N, Kuroiwa A. Hox proteins functionally cooperate with the GC box-binding protein system through distinct domains. J Biol Chem 2003;278:30148–56.
[20] Boudreau F, Rings EH, van Wering HM, Kim RK, Swain GP, Krasinski SD, et al. Hepatocyte nuclear factor-1 alpha, GATA-4, and caudal related homeodomain protein Cdx2 interact functionally to modulate intestinal gene transcription. Implication for the developmental regulation of the sucrase-isomaltase gene. J Biol Chem 2002;277:31909–17.
[21] Mutoh H, Satoh K, Kita H, Sakamoto H, Hayakawa H, Yamamoto H, et al. Cdx2 specifies the differentiation of morphological as well as functional absorptive enterocytes of the small intestine. Int J Dev Biol 2005;49:867–71.
[22] Ogihara H, Saito H, Shin BC, Terada T, Takenoshita S, Nagamachi Y, et al. Immuno-localization of H+/peptide cotransporter in rat digestive tract. Biochem Biophys Res Commun 1996;220:848–52.
[23] Adibi SA. Regulation of expression of the intestinal oligopeptide transporter (Pept-1) in health and disease. Am J Physiol Gastrointest Liver Physiol 2003;285:G779–88.
[24] Ashida K, Katsura T, Motohashi H, Saito H, Inui K. Thyroid hormone regulates the activity and expression of the peptide transporter PEPT1 in Caco-2 cells. Am J Physiol Gastrointest Liver Physiol 2002;282:G617–23.
[25] Naruhashi K, Sai Y, Tamai I, Suzuki N, Tsuji A. Pept1 mRNA expression is induced by starvation and its level correlates with absorptive transport of cefadroxil longitudinally in the rat intestine. Pharm Res 2002;19:1417–23.
[26] Shiraga T, Miyamoto K, Tanaka H, Yamamoto H, Taketani Y, Morita K, et al. Cellular and molecular mechanisms of dietary regulation on rat intestinal H^+/peptide transporter PepT1. Gastroenterology 1999;116:354–62.
[27] Pan X, Terada T, Irie M, Saito H, Inui K. Diurnal rhythm of H^+-peptide cotransporter in the rat small intestine. Am J Physiol Gastrointest Liver Physiol 2002;283:G57–64.
[28] Fujita T, Majikawa Y, Umehisa S, Okada N, Yamamoto A, Ganapathy V, et al. σ-Receptor ligand-induced up-regulation of the H^+/peptide transporter PEPT1 in the human intestinal cell line Caco-2. Biochem Biophys Res Commun 1999;261:242–6.

0022-3565/06/3181-455–460$20.00
THE JOURNAL OF PHARMACOLOGY AND EXPERIMENTAL THERAPEUTICS
Copyright © 2006 by The American Society for Pharmacology and Experimental Therapeutics
JPET 318:455–460, 2006

Vol. 318, No. 1
102830/3120199
Printed in U.S.A.

Transport Characteristics of a Novel Peptide Transporter 1 Substrate, Antihypotensive Drug Midodrine, and Its Amino Acid Derivatives

Masahiro Tsuda, Tomohiro Terada, Megumi Irie, Toshiya Katsura, Ayumu Niida, Kenji Tomita, Nobutaka Fujii, and Ken-ichi Inui

Department of Pharmacy, Kyoto University Hospital, Faculty of Medicine (M.T., T.T., M.I., T.K., K.I.), and Graduate School of Pharmaceutical Science (A.N., K.T., N.F.), Kyoto University, Kyoto, Japan

Received February 12, 2006; accepted April 4, 2006

ABSTRACT

Midodrine is an oral drug for orthostatic hypotension. This drug is almost completely absorbed after oral administration and converted into its active form, 1-(2′,5′-dimethoxyphenyl)-2-aminoethanol) (DMAE), by the cleavage of a glycine residue. The intestinal H^+-coupled peptide transporter 1 (PEPT1) transports various peptide-like drugs and has been used as a target molecule for improving the intestinal absorption of poorly absorbed drugs through amino acid modifications. Because midodrine meets these requirements, we examined whether midodrine can be a substrate for PEPT1. The uptake of midodrine, but not DMAE, was markedly increased in PEPT1-expressing oocytes compared with water-injected oocytes. Midodrine uptake by Caco-2 cells was saturable and was inhibited by various PEPT1 substrates. Midodrine absorption from the rat intestine was very rapid and was significantly inhibited by the high-affinity PEPT1 substrate cyclacillin, assessed by the alteration of the area under the blood concentration-time curve for 30 min and the maximal concentration. Some amino acid derivatives of DMAE were transported by PEPT1, and their transport was dependent on the amino acids modified. In contrast to neutral substrates, cationic midodrine was taken up extensively at alkaline pH, and this pH profile was reproduced by a 14-state model of PEPT1, which we recently reported. These findings indicate that PEPT1 can transport midodrine and contributes to the high bioavailability of this drug and that Gly modification of DMAE is desirable for a prodrug of DMAE.

H^+-coupled peptide transporter 1 (PEPT1) expressed in the brush-border membranes of intestinal epithelial cells transports dipeptides and tripeptides from the lumen into cells using an inward H^+-electrochemical gradient (Inui and Terada, 1999; Daniel, 2004; Terada and Inui, 2004). In addition to dipeptides and tripeptides, various peptide-like drugs, such as oral β-lactam antibiotics, can be transported by PEPT1; therefore, PEPT1 serves as a drug transporter (Yang et al., 1999; Daniel and Kottra, 2004; Terada and Inui, 2004). Over the last decade, PEPT1 has been used as a target molecule for improving the intestinal absorption of poorly absorbed drugs through amino acid modifications. For example, the enhanced oral bioavailability of valacyclovir and valganciclovir, amino acid ester prodrugs of acyclovir and ganciclovir, respectively, has been attributed to their enhanced intestinal transport via PEPT1 (Han et al., 1998; Sugawara et al., 2000).

Midodrine is a selective α1-receptor agonist to treat orthostatic hypotension and is a prodrug of 1-(2′,5′-dimethoxyphenyl)-2-aminoethanol (DMAE) to combine the glycine by a peptide bond. After oral administration, the bioavailability of midodrine is reported to be approximately 100%, whereas that of DMAE is approximately 50%. However, mechanisms of improving intestinal absorption of midodrine have not been elucidated.

Midodrine resembles a dipeptide in structure, and improving the intestinal absorption of DMAE by modifying an amino acid is similar to the relationship between acyclovir and valacyclovir. Based on this background, in the present study, we examined whether midodrine can be a substrate for PEPT1 in vitro and in vivo. Furthermore, we synthesized various DMAE amino acid derivatives to clarify which amino

This work was supported by the 21st Century Center of Excellence Program "Knowledge Information Infrastructure for Genome Science," the Leading Project for Biosimulation, a grant-in-aid for Scientific Research from the Ministry of Education, Culture and Sports of Japan, and a grant-in-aid for Research on Advanced Medical Technology from the Ministry of Health, Labor and Welfare of Japan.

Article, publication date, and citation information can be found at http://jpet.aspetjournals.org.

doi:10.1124/jpet.106.102830.

ABBREVIATIONS: PEPT1, H^+-coupled peptide transporter 1; DMAE, 1-(2′,5′-dimethoxyphenyl)-2-aminoethanol; MES, 2-(*N*-morpholino)ethanesulfonic acid; HPLC, high-performance liquid chromatography; TFA, trifluoroacetic acid; AUC, area under the curve.

acid modification by a peptide bond is the most suitable for interaction with PEPT1 using DMAE as a model compound. We do not have enough information regarding this issue, although there are various reports to examine the interaction of amino acid esterification of poorly absorbed drugs with PEPT1 (Han et al., 1998; Sawada et al., 1999). Finally, we simulated pH profiles of midodrine (cationic) and a glutamate derivative of DMAE (neutral) using a 14-state model of PEPT1, which we constructed recently (Irie et al., 2005).

Materials and Methods

Materials. Midodrine and DMAE were gifts from Taisho Pharmaceutical (Tokyo, Japan). [^{3}H]Glycylsarcosine (4 Ci/mmol) was obtained from Moravek Biochemicals Inc. (Brea, CA). Glycylsarcosine was purchased from Sigma Chemical Co. (St. Louis, MO). All other chemicals used were of the highest purity available.

DMAE Amino Acid Derivatives Synthesis. Figure 1 shows the structures of DMAE amino acid derivatives. The derivatives were obtained as follows. Diisopropylethylamine (1 Eq), *N*-Boc-protected amino acid (1 Eq) [side chain protection: Tyr (*t*-Bu); Cys (Trt); Lys (Boc); and Glu (*t*-Bu)], HOBt·H_2O (1 Eq), and WSCDI (1 Eq) were added to a solution of DMAE hydrochloride in dimethylformamide at 0°C. The mixture was stirred for 12 h at room temperature and extracted with ethyl acetate. The extract was washed with saturated citric acid, saturated $NaHCO_3$, and brine and dried over $MgSO_4$. Concentration under reduced pressure followed by flash chromatography over silica gel gave the amide compound. Deprotection of the resulting amide with 4 M HCl-dioxane for 2 h at room temperature followed by purification through reversed-phase-HPLC (H_2O-CH_3CN containing 0.1% TFA) gave the desired midodrine derivative (1:1 mixture of diastereomers) as TFA salts (two steps, ~50–80% yield). All compounds were characterized by ^{1}H NMR and electrospray ionization-mass spectrometry.

Cell Culture. Caco-2 cells obtained from the American Type Culture Collection (ATCC HTB37) were maintained by serial passage in plastic culture dishes as described previously (Irie et al., 2001). To measure the uptake of midodrine from the apical side, Caco-2 cells were seeded on 35-mm plastic dishes (2×10^5 cells/dish, 2 ml of culture medium). The cell monolayers were given fresh culture medium every 2 to 4 days and were used on the 14th or 15th day for experiments.

Uptake Experiments with Cell Monolayers. The uptake of [^{3}H]glycylsarcosine was measured as described previously (Terada et al., 1997). In experiments using midodrine, DMAE, and DMAE amino acid derivatives, the extraction solution (water/acetonitrile, 50:50) was added to the cells after the uptake period. On standing for 1 h at room temperature, the solutions were centrifuged and the supernatants were filtered through a Millipore filter (SGJVL, 0.22 μm; Millipore Corporation, Billerica, MA). The filtrates were analyzed by HPLC. Because midodrine and DMAE amino acid derivatives were partially metabolized to DMAE and each amino acid within Caco-2 cells and oocytes, the amounts of midodrine and

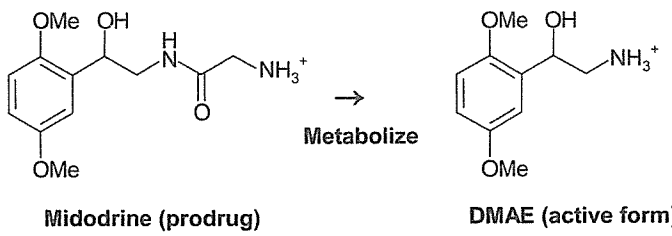

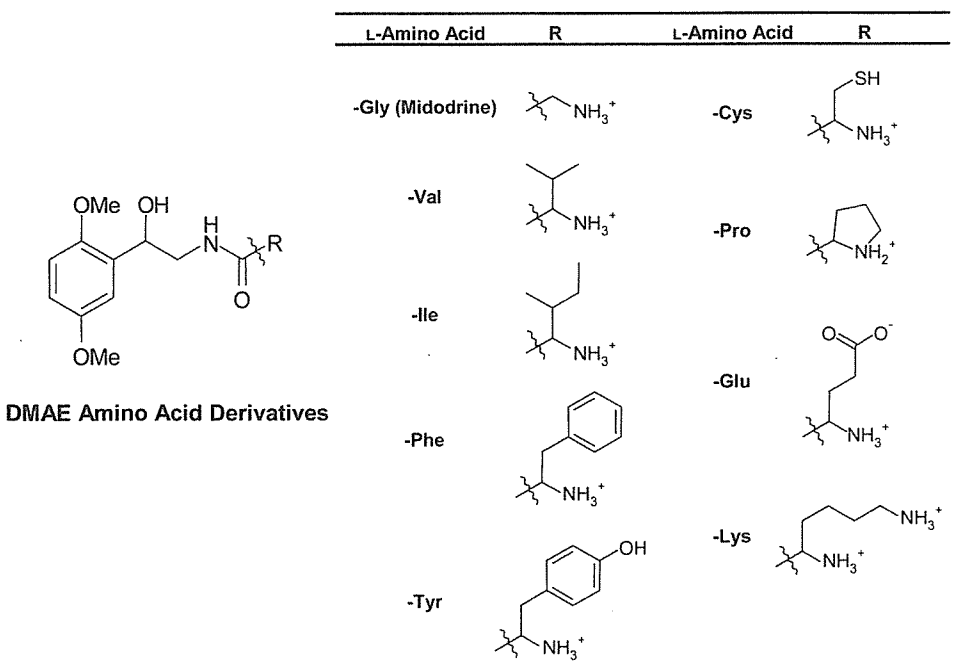

Fig. 1. Structures of midodrine, DMAE, and DMAE amino acid derivatives.

DMAE amino acid derivatives taken up were calculated as the sum of the amounts of the unchanged form and DMAE.

Simulation. A 14-state model of PEPT1, which we recently constructed (Irie et al., 2005), was used to simulate the pH profiles of midodrine and glutamate derivative of DMAE.

Uptake Experiments with *Xenopus* Oocytes. The synthesis and injection of cRNA were performed as described previously (Terada et al., 1996). The uptake of midodrine and DMAE was examined as reported with slight modifications (Saito et al., 1995). In brief, the uptake reaction was initiated in a 24-well plate by incubating the oocytes in 500 μl of uptake buffer, pH 6.0 (96 mM NaCl, 2 mM KCl, 1.8 mM $CaCl_2$, 1 mM $MgCl_2$, and 5 mM MES, pH 6.0, or HEPES, pH 7.4) containing 1 mM midodrine or DMAE for 1 h at room temperature. At the end of the uptake period, oocytes were washed five times in 1.5 ml of ice-cold uptake buffer, pH 7.4, and were transferred to a 1.5-ml tube. The oocytes were homogenized in 0.2 ml of extraction solution (water/acetonitrile, 50:50). The homogenates were centrifuged at 10,000 rpm for 5 min, and supernatants were filtered through a Millipore filter SGJVL (0.45 μM). The filtrates were analyzed by HPLC.

In Vivo Experiments. Experiments in vivo were performed as described previously (Pan et al., 2003). In brief, rats were anesthetized with sodium pentobarbital (50 mg/kg). The femoral artery was cannulated with a polyethylene tube (SP-31; Natsume Seisakusho, Tokyo, Japan) for blood sampling. For the intraintestinal administration of midodrine, the abdominal cavity of rats was opened via a midline incision, and the upper site of the duodenum was exposed to administer the drug. Midodrine was injected into the lumen of the duodenum at a dose of 2.91 mg/kg. Blood samples were collected from the femoral artery at 1, 5, 10, 15, 30, 45, 60, 90, and 120 min after the end of the injection. The blood samples were centrifuged at 14,000 rpm for 3 min, and 100 μl of plasma was deproteinized by adding 200 μl of methanol. The samples were centrifuged at 14,000 rpm for 3 min, and supernatants were filtered through a Millipore filter (SGJVL, 0.45 μm). The filtrates were analyzed by HPLC.

Analytical Methods. The uptake of midodrine and DMAE by Caco-2 cells and oocytes was measured simultaneously using high-performance liquid chromatograph LC-10AD_{SP} (Shimadzu Co., Kyoto, Japan) equipped with an SPD-10A_{VP} variable wavelength UV detector (Shimadzu Co.) and an integrator (Chromatopac C-R8A; Shimadzu Co.) under the following conditions: column, TSK-gel ODS 80TM (4.6 mm i.d. × 150; Tosoh Co., Tokyo, Japan); mobile phase, 1% SDS/phospholic acid/acetonitrile, 600:1:400; flow rate, 0.8 ml/min; wavelength, 290 nm; injection volume, 50 μl; and temperature, 50°C for midodrine, DMAE, and DMAE amino acid derivatives, except for a lysyl derivative of DMAE: mobile phase, water, and acetonitrile, both containing 0.1% (v/v) TFA, linear gradient of acetonitrile in water 10 to 40% over 30 min; flow rate, 1.0 ml/min; wavelength, 220 nm; injection volume, 50 μl; and temperature, 40°C for a lysyl derivative of DMAE.

Data Analysis. Each experimental point represents the mean ± S.E. of three to nine measurements from one to three separate experiments. Data from uptake experiments were analyzed statistically by a one-way analysis of variance followed by Sheffé's test. Kinetic parameters of the DMAE plasma concentration were statistically compared using a nonpaired t test.

Results

Effect of Midodrine on [^{3}H]Glycylsarcosine Uptake by Caco-2 Cells. To assess the interaction of midodrine with PEPT1, we examined the inhibitory effect of midodrine on [^{3}H]glycylsarcosine uptake by Caco-2 cells. As shown in Fig. 2A, [^{3}H]glycylsarcosine uptake was inhibited by midodrine in a concentration dependent manner, and the IC_{50} value was calculated at 2.8 ± 0.1 mM.

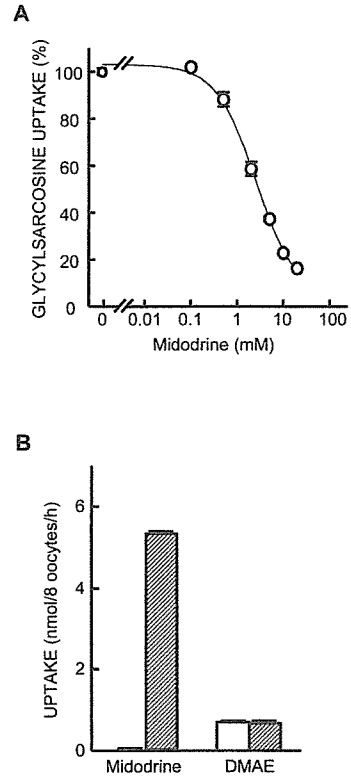

Fig. 2. A, effect of midodrine on [^{3}H]glycylsarcosine uptake by Caco-2 cells. The cell monolayers were incubated at 37°C for 15 min with 25 μM [^{3}H]glycylsarcosine, pH 6.0, in the presence of various concentrations of midodrine. After the incubation, the radioactivity of dissolved cells was measured. Each point represents the mean ± S.E. of three independent monolayers. The IC_{50} value was calculated from three separate experiments. B, uptake of midodrine and DMAE by oocytes expressing PEPT1. Water-injected (open column) or PEPT1-expressing (hatched column) oocytes were incubated at 37°C for 1 h with 1 mM midodrine or DMAE, pH 6.0. The amounts of midodrine and DMAE in the solubilized oocytes were measured by HPLC. Each column represents the mean ± S.E. of three experiments. Each experiment was performed with eight oocytes.

Uptake of Midodrine and DMAE by Oocytes Expressing PEPT1. To confirm the midodrine transport by PEPT1, we measured the uptake of midodrine and DMAE by PEPT1-expressing oocytes. As shown in Fig. 2B, the uptake of midodrine was markedly increased in PEPT1-expressing oocytes compared with water-injected oocytes. In contrast, no PEPT1-mediated transport of DMAE was observed.

Uptake of Midodrine and DMAE by Caco-2 Cells. To investigate the transport and metabolism of midodrine in the intestinal epithelial cells, uptake experiments were performed using Caco-2 cells. Figure 3A shows the time course of midodrine and DMAE uptake by Caco-2 cells. As shown in Fig. 3A, more midodrine than DMAE was taken up at each time point. After 1 h of incubation in Caco-2 cells, ~35% midodrine was metabolized to DMAE (Fig. 3B)

Transport Characteristics of Midodrine in Caco-2 Cells. Figure 4A shows the effect of various compounds on midodrine uptake in Caco-2 cells. PEPT1-dependent part of midodrine uptake was nearly completely inhibited by PEPT1 substrates, but not by glycine. As shown in Fig. 4B, midodrine uptake by Caco-2 cells was saturable, and the apparent Michaelis-Menten constant (K_m) value was calculated at 4.5 ± 1.3 mM.

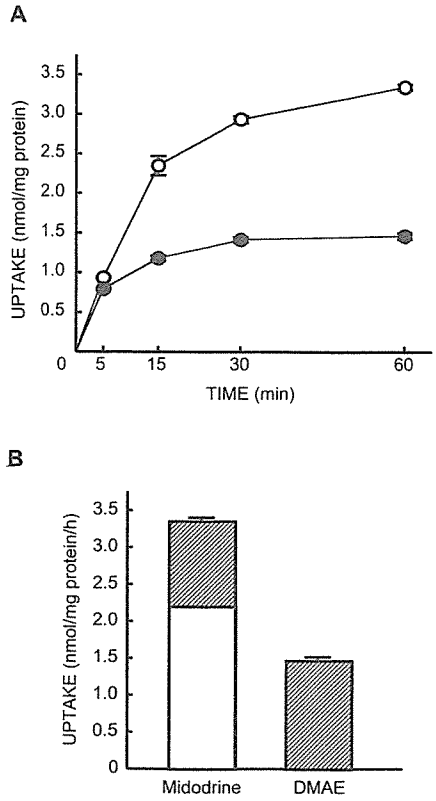

Fig. 3. A, time course of midodrine and DMAE uptake by Caco-2 cells. The cell monolayers were incubated at 37°C for the periods indicated with 0.5 mM midodrine or DMAE, pH 6.0. After the incubation, the amounts of midodrine (○) and DMAE (●) extracted from the cell monolayers were measured by HPLC. Each point represents the mean ± S.E. of three independent monolayers. B, metabolism of midodrine in Caco-2 cells after 1-h uptake. Open and hatched columns represent midodrine and DMAE, respectively. Each column represents the mean ± S.E. of three independent monolayers.

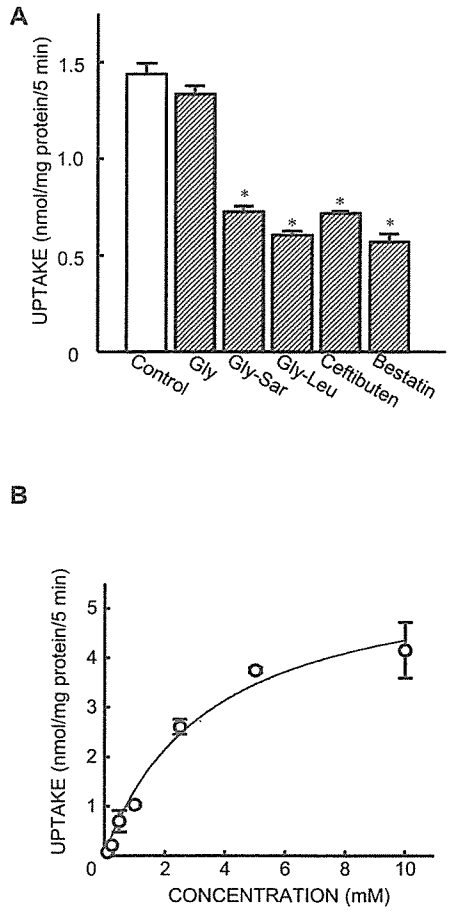

Fig. 4. A, effect of various compounds on midodrine uptake by Caco-2 cells. The cell monolayers were incubated at 37°C for 5 min with 0.5 mM midodrine, pH 6.0, in the absence or presence of each inhibitor (10 mM). After the incubation, the amounts of midodrine and DMAE extracted from the cell monolayers were measured by HPLC. Each column represents the mean ± S.E. of three independent monolayers. *, $P < 0.05$, significantly different from the control. B, concentration dependence of midodrine uptake by Caco-2 cells. Nonspecific uptake was evaluated by measuring midodrine uptake in the presence of 50 mM glycylleucine, and the results are shown after correction for the nonsaturable component. The cell monolayers were incubated at 37°C for 5 min with various concentration of midodrine, pH 6.0. After the incubation, the amounts of midodrine and DMAE extracted from the cell monolayers were measured by HPLC. Each point represents the mean ± S.E. of three independent monolayers. The K_m value was calculated from three separate experiments.

Absorption of Midodrine from Rat Intestine. To confirm the involvement of PEPT1 in the transport of midodrine in vivo, we performed a pharmacokinetic analysis. Figure 5 shows the time course of DMAE plasma concentration after the intraintestinal administration of midodrine in rats. The concentration peaked 5 min after the intraintestinal administration, indicating that the absorption of midodrine was very rapid. Midodrine absorption was inhibited in the presence of cyclacillin, a high-affinity substrate of PEPT1, until 30 min postadministration. The estimated pharmacokinetic parameters are summarized in Table 1. The area under the blood concentration-time curve for 30 min (AUC_{0-30}) and the maximal concentration in the presence of cyclacillin were reduced significantly compared with the control values, and the time to maximal concentration (t_{max}) was significantly longer than the control.

Uptake of DMAE Amino Acid Derivatives in Caco-2 Cells. To examine which amino acid modification of midodrine is suitable for interaction with PEPT1, we synthesized various DMAE-L-amino acid derivatives DMAE-X (X: -Val, -Ile, -Phe, -Tyr, -Cys, -Pro, -Glu, and -Lys), in which the glycine residue is replaced by other amino acids (Fig. 1). We measured the uptake of these derivatives in Caco-2 cells in the absence or presence of the excess glycylsarcosine (Fig. 6). DMAE-Phe uptake was greatest but was not inhibited by the glycylsarcosine. DMAE-Val, -Ile, -Tyr, -Cys, -Glu, and -Lys uptake was roughly equal to midodrine uptake, but the excess glycylsarcosine did not have a significant inhibitory effect in the case of DMAE-Ile and -Lys. DMAE-Pro uptake by Caco-2 cells was low and not inhibited by the excess glycylsarcosine. Furthermore, using in vitro everted sacs of the rat small intestine, we examined the stability of three kinds of derivatives (DMAE-Gly, -Val, and -Phe) at the mucosal surface. The ratio of unchanged form at the mucosal side after 1 h of incubation was as follows: DMAE-Gly (95%), -Val (47%), and -Phe (0.7%), suggesting that DMAE-Gly (midodrine) is the most stable derivative among the tested compounds.

pH Dependence of Midodrine and DMAE-Glu Uptake by Caco-2 Cells. Figure 7A shows the pH dependence of midodrine and DMAE-Glu uptake by Caco-2 cells. In contrast

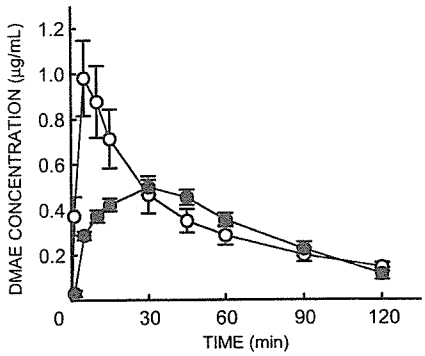

Fig. 5. DMAE plasma concentration after intraintestinal administration in the absence or presence of cyclacillin. After intraintestinal administration at a dose of 2.91 mg/kg midodrine and in the absence (○) or presence (●) of 6.85 mg/kg cyclacillin, blood samples were collected at the times indicated. The blood samples were determined by HPLC. Each point represents the mean ± S.E. of six rats.

TABLE 1

Pharmacokinetic parameters of the DMAE plasma concentration in the absence or presence of cyclacillin after intraintestinal administration

Each value represents the mean ± S.E. of six rats.

	$AUC_{0-30\ min}$	$AUC_{0-120\ min}$	C_{max}	t_{max}
	μg·min/ml		*μg/ml*	*min*
Control	20.4 ± 3.5	43.6 ± 7.0	1.01 ± 0.18	5.8 ± 0.8
+Cyclacillin	11.3 ± 0.7*	38.1 ± 3.0	0.51 ± 0.03*	35.0 ± 3.2*

C_{max}, maximal concentration.
*$P < 0.01$, significantly different from the control.

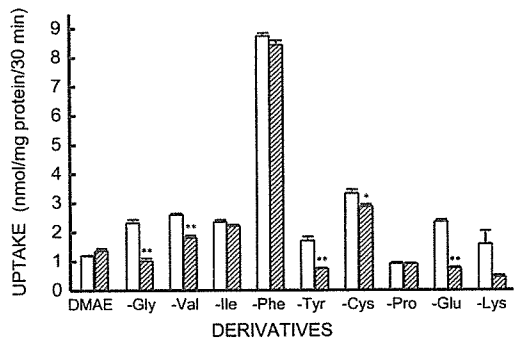

Fig. 6. Uptake of DMAE amino acid derivatives in Caco-2 cells. The cell monolayers were incubated at 37°C for 30 min with 0.5 mM of each DMAE amino acid derivative in the absence (opened column) or presence (hatched column) of 10 mM glycylsarcosine. After the incubation, the amounts of DMAE amino acid derivatives extracted from the cell monolayers were measured by HPLC. Each column represents the mean ± S.E. of three independent monolayers. *, $P < 0.05$; **, $P < 0.01$, significantly different from the control.

to neutral substrates, the cationic midodrine was taken up extensively at alkaline pH. This pH profile was similar to that of the cationic dipeptides transported by PEPT1 (Mackenzie et al., 1996). On the other hand, the pH dependence of DMAE-Glu (neutral) uptake was high at acidic pH. Recently, we constructed a 14-state model of PEPT1 and reproduced the pH profiles of various charged substrates (Irie et al., 2005). The pH profile of midodrine as well as DMAE-Glu was reproduced by our 14-state model of PEPT1 (Fig. 7B). In the simulation, the uptake of midodrine and DMAE-Glu was calculated every 0.01 pH units. Four dissociation constants of midodrine and DMAE-Glu on the exterior side

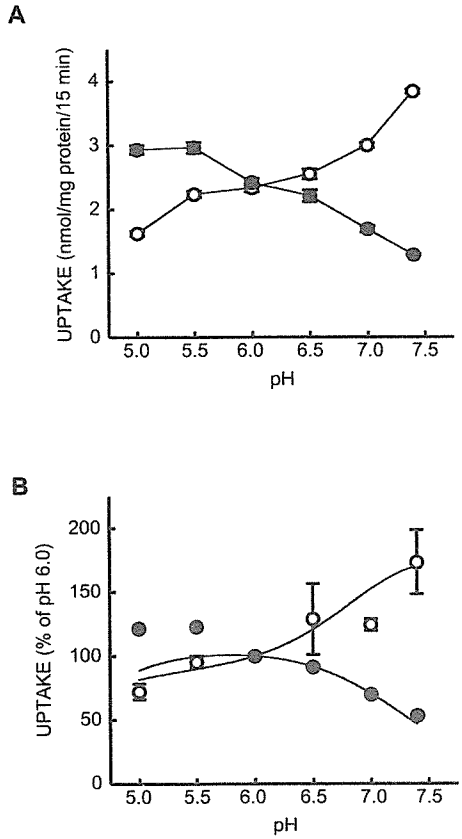

Fig. 7. A, pH dependence of midodrine (○) and DMAE-Glu (●) uptake by Caco-2 cells. The cell monolayers were incubated at 37°C for 15 min with 0.5 mM midodrine or DMAE-Glu, pH 6.0. After the incubation, the amounts of midodrine, DMAE-Glu, and DMAE extracted from the cell monolayers were measured by HPLC. Each point represents the mean ± S.E. of three independent monolayers. B, simulation of pH dependence of midodrine (○) and DMAE-Glu (●) uptake by Caco-2 cells. The rates of uptake value at pH 6.0 were derived from the uptake values in Fig. 6A. The pH profiles of midodrine and DMAE-Glu uptake were delineated by simulation (curve). Four dissociation constants (in micromolars) of midodrine and DMAE-Glu on the exterior side ($K_{d,\ Soc1}$, $K_{d,\ Soc2}$, $K_{d,\ Son}$, and $K_{d,\ Soa}$) were defined as follows: $K_{d,\ Soc1} = 1500$, $K_{d,\ Soc2} = 120$, $K_{d,\ Son} = 2000$, $K_{d,\ Soa} = 2000$, $K_{d,\ Soc1} = 500$, $K_{d,\ Soc2} = 500$, $K_{d,\ Son} = 300$, and $K_{d,\ Soa} = 2000$, respectively.

($K_{d,\ Soc1}$, $K_{d,\ Soc2}$, $K_{d,\ Son}$, and $K_{d,\ Soa}$) were recalculated based on our 14-state model (Irie et al., 2005).

Discussion

Midodrine is an oral drug that acts as a selective α1-receptor agonist and the medication of choice for treating orthostatic hypotension in the elderly (Mukai and Lipsitz, 2002). Furthermore, this drug is beneficial in preventing or ameliorating the symptoms of intradialytic hypotension (Prakash et al., 2004). There are many reports regarding the pharmacological and clinical effects of midodrine, but its pharmacokinetic properties, especially the mechanism behind its intestinal absorption, have not been elucidated. In the present study, we demonstrated for the first time that midodrine was transported by PEPT1 in vitro and in vivo. Because PEPT1 can transport various peptide-like drugs, such as β-lactam antibiotics and antiviral drugs, and also mediates the cellular uptake of dipeptides and tripeptides derived from ingested proteins, there is potential for drug/

drug interaction and/or drug/food interaction during therapy with midodrine.

Previously, Beauchamp et al. (1992) evaluated the bioavailability of 18 ester compounds of acyclovir and found that the L-valyl ester derivative had the best bioavailability followed by the L-isoleucyl, L-alanyl, and glycyl ester derivatives. Thereafter, these amino acid preferences were demonstrated to be related to the affinity for PEPT1 (Sawada et al., 1999). Thus, for amino acid ester modification, L-valine may be a suitable target for converting a poorly absorbed drug into a substrate of PEPT1. On the other hand, for amino acid modification of a peptide bond, there is little information available on which amino acids provide for high-affinity interaction with PEPT1 and resistance against enzymatic degradation. In the present study, we demonstrated that the derivatives with -Gly, -Val, -Tyr, -Cys, and -Glu were suggested to be interacted with PEPT1, but those with -Ile, -Phe, -Pro, and -Lys did not (the lack of significant difference in the case of -Lys may be caused by the unusually high scatter). Large amounts of DMAE-Phe were accumulated in Caco-2 cells, but this derivative showed extremely low stability in the rat small intestine. These findings suggest that DMAE-Phe may not be appropriate for a prodrug for targeting PEPT1 and improving the intestinal absorption in vivo. On the other hand, DMAE-Gly (midodrine) was high stability and can be recognized by PEPT1. Although we did not perform a detailed analysis, overall, our results suggest that Gly modification of DMAE by a peptide bond is appropriate for the preparation of a prodrug for DMAE. Further studies are needed to define the amino acids suitable for targeting PEPT1 in peptide bond-based modifications.

It has been reported that pH dependences of neutral (Inui et al., 1992; Saito and Inui, 1993; Terada et al., 1999; Kennedy et al., 2002) and anionic (Matsumoto et al., 1995) substrates of PEPT1 show different profiles. The pH dependence of cationic substrates determined by measuring evoked current is also different from neutral and anionic substrates (Mackenzie et al., 1996). Midodrine almost exists as a cation at pH 5.0 to 7.4, because its dissociation constant (p*K*a) is 7.96. As shown in Fig. 7A, midodrine uptake by PEPT1 gradually increased as the pH rose from 5.0 to 7.4. This pH profile clearly differs from that of a neutral substrate, such as glycylsarcosine, or an anionic substrate, such as ceftibuten. In contrast, the pH profile of DMAE-Glu, which mainly exists as a neutral substrate from pH 5.0 to 7.4, was similar to that of glycylsarcosine. Recently, based on the presumed recognition patterns of PEPT1 for neutral and charged substrates, we constructed a 14-state model of PEPT1 and reproduced the pH profiles of various charged substrates (Irie et al., 2005). In this model, we hypothesized two mechanisms for the transport of cationic substrates, namely, that the transport of cationic substrate occurs with or without H^+. Therefore, the transport of cationic substrates is assumed to be altered by the degree of contribution of the two pathways. In the previous study, we could not simulate the pH profile of cationic substrates, because there is little known regarding the transport characteristics of cationic substrates of PEPT1. The present simulation revealed that the pH profile of midodrine as well as DMAE-Glu was reproduced by our 14-state model of PEPT1 (Fig. 7B), suggesting that our model can be applied to cationic as well as neutral substrates.

In conclusion, we have demonstrated that midodrine, but not DMAE, is recognized by PEPT1 and that this recognition improves the oral bioavailability of DMAE. In addition, the transport of DMAE amino acid derivatives via PEPT1 depends on the amino acids modified. These findings suggested that modifying not only the L-valyl ester but also the glycyl peptide of poorly absorbed drugs, which are targeted to intestinal PEPT1, is useful for improving of the intestinal absorption of drugs.

References

Beauchamp LM, Orr GF, de Miranda P, Burnette T, and Krenitsky (1992) Amino acid ester prodrugs of acyclovir. *Antiviral Chem Chemother* **3**:157–164.

Daniel H (2004) Molecular and integrative physiology of intestinal peptide transport. *Annu Rev Physiol* **66**:361–384.

Daniel H and Kottra G (2004) The proton oligopeptide cotransporter family SLC15 in physiology and pharmacology. *Pflueg Arch Eur J Physiol* **447**:610–618.

Han H, de Vrueh RL, Rhie JK, Covitz KM, Smith PL, Lee CP, Oh DM, Sadée W, and Amidon GL (1998) 5′-Amino acid esters of antiviral nucleosides, acyclovir and AZT are absorbed by the intestinal PEPT1 peptide transporter. *Pharm Res (NY)* **15**: 1154–1159.

Inui K and Terada T (1999) Dipeptide transporters, in *Membrane Transporters as Drug Targets* (Amidon GL and Sadée W eds) pp 269–288, Academic/Plenum Publishers, New York.

Inui K, Yamamoto M, and Saito H (1992) Transepithelial transport of oral cephalosporins by monolayers of intestinal epithelial cell line Caco-2: specific transport systems in apical and basolateral membranes. *J Pharmacol Exp Ther* **261**:195–201.

Irie M, Terada T, Katsura T, Matsuoka S, and Inui K (2005) Computational modeling of H^+-coupled peptide transport via human PEPT1. *J Physiol (Lond)* **565**:429–439.

Irie M, Terada T, Sawada K, Saito H, and Inui K (2001) Recognition and transport characteristics of nonpeptidic compounds by basolateral peptide transporter in Caco-2 cells. *J Pharmacol Exp Ther* **298**:711–717.

Kennedy DJ, Leibach FH, Ganapathy V, and Thwaites DT (2002) Optimal absorptive transport of the dipeptide glycylsarcosine is dependent on functional Na^+/H^+ exchange activity. *Pflueg Arch Eur J Physiol* **445**:139–146.

Mackenzie B, Fei YJ, Ganapathy V, and Leibach FH (1996) The human intestinal H^+/oligopeptide cotransporter hPEPT1 transports differently-charged dipeptides with identical electrogenic properties. *Biochim Biophys Acta* **1284**:125–128.

Matsumoto S, Saito H, and Inui K (1995) Transport characteristics of ceftibuten, a new cephalosporin antibiotic, via the apical H^+/dipeptide cotransport system in human intestinal cell line Caco-2: regulation by cell growth. *Pharm Res (NY)* **12**:1483–1487.

Mukai S and Lipsitz LA (2002) Orthostatic hypotension. *Clin Geriatr Med* **18**:253–268.

Pan X, Terada T, Okuda M, and Inui K (2003) Altered diurnal rhythm of intestinal peptide transporter by fasting and its effects on the pharmacokinetics of ceftibuten. *J Pharmacol Exp Ther* **307**:626–632.

Prakash S, Garg AX, Heidenheim AP, and House AA (2004) Midodrine appears to be safe and effective for dialysis-induced hypotension: a systematic review. *Nephrol Dial Transplant* **19**:2553–2558.

Saito H and Inui K (1993) Dipeptide transporters in apical and basolateral membranes of the human intestinal cell line Caco-2. *Am J Physiol* **265**:G289–G294.

Saito H, Okuda M, Terada T, Sasaki S, and Inui K (1995) Cloning and characterization of a rat H^+/peptide cotransporter mediating absorption of beta-lactam antibiotics in the intestine and kidney. *J Pharmacol Exp Ther* **275**:1631–1637.

Sawada K, Terada T, Saito H, Hashimoto Y, and Inui K (1999) Recognition of L-amino acid ester compounds by rat peptide transporters PEPT1 and PEPT2. *J Pharmacol Exp Ther* **291**:705–709.

Sugawara M, Huang W, Fei YJ, Leibach FH, Ganapathy V, and Ganapathy ME (2000) Transport of valganciclovir, a ganciclovir prodrug, via peptide transporters PEPT1 and PEPT2. *J Pharm Sci* **89**:781–789.

Terada T and Inui K (2004) Peptide transporters: structure, function, regulation, and application for drug delivery. *Curr Drug Metab* **5**:85–94.

Terada T, Saito H, Mukai M, and Inui K (1996) Identification of the histidine residues involved in substrate recognition by a rat H^+/peptide cotransporter, PEPT1. *FEBS Lett* **394**:196–200.

Terada T, Saito H, Mukai M, and Inui K (1997) Recognition of beta-lactam antibiotics by rat peptide transporters, PEPT1 and PEPT2, in LLC-PK_1 cells. *Am J Physiol* **273**:F706–F711.

Terada T, Sawada K, Saito H, and Inui K (1999) Functional characteristics of basolateral peptide transporter in the human intestinal cell line Caco-2. *Am J Physiol* **276**:G1435–G1441.

Yang CY, Dantzig AH, and Pidgeon C (1999) Intestinal peptide transport systems and oral drug availability. *Pharm Res (NY)* **16**:1331–1343.

Address correspondence to: Professor Ken-ichi Inui, Department of Pharmacy, Kyoto University Hospital, Sakyo-ku, Kyoto 606-8507, Japan. E-mail: inui@kuhp.kyoto-u.ac.jp

The PDZ domain protein PDZK1 interacts with human peptide transporter PEPT2 and enhances its transport activity

R Noshiro[1,2,4], N Anzai[1,4], T Sakata[1,2], H Miyazaki[1], T Terada[3], HJ Shin[1], X He[1], D Miura[1], K Inui[3], Y Kanai[1] and H Endou[1,2]

[1]*Department of Pharmacology and Toxicology, Kyorin University School of Medicine, Mitaka, Tokyo, Japan;* [2]*Fuji Biomedix Co. Ltd, Chuo-ku, Tokyo, Japan and* [3]*Department of Pharmacy, Kyoto University Hospital, Sakyo-ku, Kyoto, Japan*

The proton-coupled peptide transporter PEPT2 (*SLC15A2*) mediates the high-affinity low-capacity transport of small peptides as well as various oral peptide-like drugs in the kidney. In contrast to its well-characterized transport properties, there is less information available on its regulatory mechanism, although the interaction of PEPT2 to the PDZ (PSD-95, DglA, and ZO-1)-domain protein PDZK1 has been preliminarily reported. To examine whether PDZK1 is a physiological partner of PEPT2 in kidneys, we started from a yeast two-hybrid screen of a human kidney cDNA library with the C-terminus of PEPT2 (PEPT2 C-terminus (PEPT2-CT)) as bait. We could identify PDZK1 as one of the positive clones. This interaction requires the PDZ motif of PEPT2-CT detected by a yeast two-hybrid assay, *in vitro* binding assay and co-immunoprecipitation. The binding affinities of second and third PDZ domains of PDZK1 to PEPT2-CT were measured by surface plasmon resonance. Co-immunoprecipitation using human kidney membrane fraction and localization of PEPT2 in renal apical proximal tubules revealed the physiological meaning of this interaction in kidneys. Furthermore, we clarified the mechanism of enhanced glycylsarcosine (Gly-Sar) transport activity in PEPT2-expressing HEK293 cells after the PDZK1 coexpression. This augmentation was accompanied by a significant increase in the V_{max} of Gly-Sar transport via PEPT2 and it was also associated with the increased surface expression level of PEPT2. These results indicate that the PEPT2–PDZK1 interaction thus plays a physiologically important role in both oligopeptide handling as well as peptide-like drug transport in the human kidney.

Kidney International (2006) **70,** 275–282. doi:10.1038/sj.ki.5001522; published online 31 May 2006

KEYWORDS: oligopeptides; oligopeptide transporter; PEPT2; PDZ; PDZK1

Correspondence: *Y Kanai, Department of Pharmacology and Toxicology, Kyorin University School of Medicine, 6-20-2 Shinkawa, Mitaka, Tokyo 181-8611, Japan. E-mail: ykanai@kyorin-u.ac.jp*

[4]These authors contributed equally to this work.

Received 6 August 2005; revised 21 February 2006; accepted 8 March 2006; published online 31 May 2006

Proton-coupled peptide transporters play an important role in the maintenance of nutrition by mediating the transport of di- and tripeptides across the brush border (apical) membranes of the small intestine and kidney. In addition, peptide transporters function as drug transporters for peptide-like drugs, including β-lactam antibiotics and angiotensin converting enzyme inhibitors.[1–3] Two proton-coupled oligopeptide transporters, PEPT1 and PEPT2, have previously been cloned in rabbits,[4–6] rats[7–9] and humans.[10–12] PEPT1 was thus shown to be a high-capacity, low-affinity transporter that is expressed mainly in small intestine and, to smaller extent, in kidneys. It has been shown to play an essential role in the absorption of small peptides arising from the digestion of dietary proteins. In contrast, PEPT2 was found to be a low-capacity, high-affinity transporter that is expressed in the kidneys. In rats, Pept1 and Pept2 are sequentially expressed: Pept1 is located in the early segment and Pept2 is in the late segment of the proximal tubules.[13] In addition, both Pept1 and Pept2 are localized in the apical membranes of renal proximal tubule in rats.[14,15] Although both transporters are expressed in the kidney, PEPT2 is thought to play a dominant role in the conservation of peptide-bound amino acids. Recently, Rubio-Aliaga *et al.*[16] have reported on the impaired renal reabsorption of peptide-bound amino acids in animals lacking Pept2.

Although the transport properties and characteristics of substrate recognition for PEPT2 have been well documented, there is less information available on PEPT2 regulation. Takahashi *et al.*[17] reported a pronounced upregulation of Pept2 mRNA and protein expression in 5/6 nephrectomized rats 2 weeks after surgery and the downregulation of its mRNA 16 weeks after surgery.[18] Wenzel *et al.*[19] demonstrated that the activation of signaling pathways involving protein kinase C changes the kinetic property of pig Pept2 in a renal cell line. Recently, Bravo *et al.*[20] demonstrated a strong inhibitory effect of EGF on the rat Pept2 transport capacity. However, the modulation of the PEPT2 function by its associated protein(s) still remains unclear.

In recent years, several PDZ domain proteins, such as NHERF1/EBP50, NHERF2/E3KARP, and PDZK1, have been identified in kidneys and thus have been suggested to be involved in the stabilization, targeting, and regulation of their binding partner.[21–24] The PDZ (PSD-95, DglA, and ZO-1)-binding domains have been identified in various proteins and they are considered to be modular protein–protein recognition domains that play a role in protein targeting and protein complex assembly.[25–27] This domain binds to proteins containing the tripeptide motif $(S/T)-X-\varnothing$ (X = any residue and $\varnothing$ = a hydrophobic residue) at their C-termini.[27] As Russel *et al.*[28] mentioned, PEPT2 is localized to the apical membrane and has C-terminal amino-acid sequences that match the PDZ-binding motif (T-K-L), in a manner similar to that of other apical organic anion transporters, such as MRP2/4, NPT1, Oatp1, Oat-k1/k2; thus, indicating that PEPT2 most likely binds to certain PDZ domain proteins. We have recently identified that the urate/anion exchanger URAT1, which has a PDZ motif at its C-terminus (T-Q-F), interacts with PDZK1.[29] Interestingly, both URAT1 and PEPT2 are expressed at the apical membrane of renal proximal tubules and they are considered to function in a reabsorptive pathway for endogenous organic anions (urate[30] and oligopeptides,[1–3] respectively). It is likely that these transporters bind to either the same or other PDZ domain protein(s) via its PDZ-motif.

Very recently, Kato *et al.*[31] examined the interaction between xenobiotic transporters including PEPT2, and PDZ proteins including PDZK1. PDZK1, originally identified as a protein that interacts with MAP17, a membrane-associated protein,[32] has been reported to interact with several membrane proteins through its PDZ domain.[33] Using coexpression of PEPT2 C-terminus (PEPT2-CT) and PDZK1 in yeast, a possible interaction was demonstrated in the artificial condition. Because they solely rely on data from *in vitro* binding assays and did not provide any evidence that this interaction truly occurs in proteins expressed from the endogenous tissue, we performed yeast two-hybrid screening against a human kidney cDNA library using PEPT2-CT as bait and thus characterized this interaction in order to identify PDZK1 as a physiological binding partner of PEPT2.

RESULTS

Identification of PDZK1 by yeast two-hybrid library screening

In an attempt to isolate PEPT2-interacting protein(s) from the endogenous genes, we performed yeast two-hybrid screening against a cDNA library constructed from the human adult kidney using the PEPT2-CT as bait. From the 8.7×10^6 transformants screened, we obtained 64 positive clones. One of these clones had a sequence identical to a portion of the human PDZK1 gene.[32] We could not detect any interactions between PEPT2-CT and any other PDZ proteins that are expressed at and/or beneath the apical membrane of proximal tubules including NHERF1/EBP50, NHERF2/E3KARP, and IKEPP[34–37] (data not shown).

C-terminal PDZ motif of PEPT2 is necessary for PDZK1 interaction

To identify the region of PEPT2 that interacts with PDZK1, we constructed three mutant baits. A bait (PEPT2-CTd3) which lacks the last three residues of PEPT2, which play a crucial role in PDZ domain recognition. Two other baits (L729A and T727A), the extreme C-terminal leucine (0 position) or threonine (−2 position) of PEPT2 was replaced by alanine, which was expected to abolish the PDZ interactions.[38] These three baits did not interact with PDZK1 (Figure 1a). Therefore, the binding through PEPT2-CT suggests that the PDZ motif of PEPT2 is the site of interaction with PDZK1.

The interaction specificity between PDZK1 and PEPT2-CT was confirmed by a yeast two-hybrid assay using a bait that had the C-terminus of another human peptide transporter, PEPT1. PDZK1 did not interact with PEPT1-CT which lacks a PDZ motif (K-Q-M) (Figure 1b).

Interaction of PDZK1 individual PDZ domains with PEPT2-CT

PDZK1 possesses four PDZ domains which facilitate the assembly of protein complexes when target proteins bind via their C-terminal PDZ motifs. To determine the possible interactions of PEPT2-CT with the PDZ domains of PDZK1, we produced prey vectors, with each containing one of the individual PDZ domains (PDZ domain 1 (PDZ1), PDZ2, PDZ3, and PDZ4) from PDZK1. The interaction with the

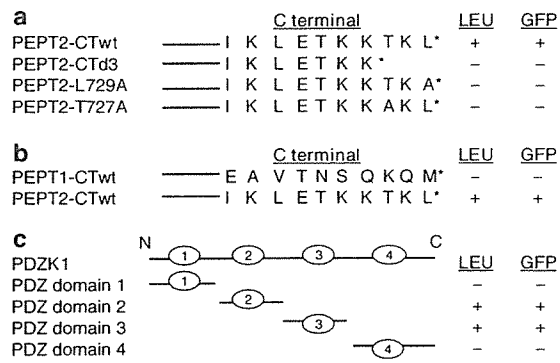

Figure 1 | Specificity of PDZK1 interaction with C-termini of PEPT2 in yeast two-hybrid system. (**a**) PDZK1 specifically interacted with the wt PEPT2 C-terminus but not with the C-terminal mutants L729A, T727A, and d727–729 (d3) of PEPT2. (**b**) Full-length PDZK1 interacting with the intracellular C-terminus of PEPT2 but not with that of PEPT1. (**c**) The wt PEPT2 C-terminus bait interacts with prey containing either the second or third PDZ domains of PDZK1 (PDZ2, PDZ3). The specificity of the prey containing a single PDZ domain of PDZK1 for the PEPT2 bait was confirmed by the absence of growth associated with the PEPT2 d3 mutant baits. The bars represent the approximate length of the baits, and the sequence of the last 10 amino acids is shown. pJG4-5 with PDZK1 cDNA expression cassette is under the control of the GAL1 promoter, such that library proteins are expressed in the presence of galactose (Gal) but not glucose (Glu). The system used for the yeast two-hybrid screen includes the reporter genes LEU2 and GFP, which replace the commonly used classical *lacZ* gene and allow a fast and easy detection of positive clones with long-wave UV. The results from the growth assay and GFP fluorescence are indicated on the right.

PEPT2-CT was observed for PDZ2 and PDZ3, but not for PDZ1 and PDZ4 of PDZK1 (Figure 1c).

In vitro binding of PEPT2 and PDZK1

We used a glutathione-*S*-transferase (GST) pull-down assay to confirm the ability of PEPT2-CT to bind to PDZK1 *in vitro* and validate the protein–protein interaction (Figure 2a). GST fusion proteins bearing the wild-type C-terminus (PEPT2-CT-wt) or C-terminal mutants (PEPT2-CTd3, L279A, and T727A) of PEPT2 were used to pull down *in vitro* translated full-length PDZK1. The data showed the same interaction specificity for PDZK1 and PEPT2 as exhibited in yeast two-hybrid assay (Figure 1a). As expected, the binding of PDZK1 to PEPT2 was completely abolished when the C-terminal PDZ motif was removed (PEPT2-CTd3) or mutated (PEPT2-CT-L729A or PEPT2-CT-T727A) (Figure 2a).

To confirm and quantify the interaction of PEPT2 with PDZK1, we performed surface plasmon resonance experiments using immobilized GST-PEPT2-CT and PDZ2 and PDZ3 of PDZK1 proteins independently fused to maltose-binding protein. As summarized in Table 1, the binding affinities of PDZ2 and PDZ3 of PDZK1 are low ($K_D = 10$ and 15 μM). These values are low in comparison to most PDZ domain interactions ($K_D = 1$ nM–10 μM).[39]

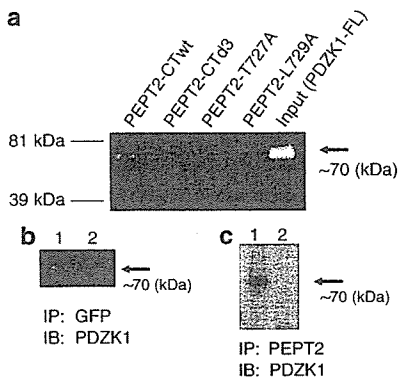

Figure 2 | Interaction of PDZK1 with PEPT2. (**a**) Full-length PDZK1 polymerase chain reaction product was *in vitro* translated in the presence of Transcend Biotinylated Lysine tRNA (Promega). The *in vitro* translation products were incubated with GST alone (lane 1), GST-PEPT2-CTwt (lane 2), or GST-PEPT2-CTd3 (lane 3) using a ProFound Pull-Down GST Protein:Protein Interaction kit (Pierce). The pull-down products were analyzed by sodium dodecyl sulfate-polyacrylamide gel electrophoresis. The input corresponds to the crude *in vitro* translation reaction. Positions of molecular mass standards are indicated on the right. GST fused to PEPT2 C-terminal wt can co-precipitate PDZK1, confirming the specificity found in the yeast two-hybrid system. The mutant form of PEPT2 in which the C-terminal PDZ recognition motif is removed is not able to precipitate PDZK1. (**b**) Co-immunoprecipitation of PEPT2 and PDZK1 in HEK293 cells. HEK293 cells were transfected with pEGFP-C2 vectors encoding PEPT2-wt (lane 1) or PEPT2-d3 (lane 2) with pcDNA3.1-PDZK1 and then immunoprecipitated with the anti-GFP antibody. Then, the immunoprecipitates were resolved by sodium dodecyl sulfate-polyacrylamide gel electrophoresis and probed with anti-PDZK1 antibodies. (**c**) Human kidney membrane fractions were immunoprecipitated with the anti-PEPT2 antibody (lane 1) and control immunoglobulin G (lane 2). The presence of PDZK1 in the immunoprecipitates was determined by Western blotting with the anti-PDZK1 antibody used in a previous study.[29]

Co-immunoprecipitation from heterologous cells and tissue

To demonstrate that PEPT2 and PDZK1 can also interact in mammalian cells, we used a previously prepared rabbit polyclonal antibody against PDZK1.[29] We coexpressed full-length human PEPT2 fused with green fluorescent protein (GFP) (GFP-PEPT2) and PDZK1 in human embryonic kidney (HEK)293 cells. Wild-type GFP-PEPT2 was co-immunoprecipitated with a GFP-specific antibody but GFP-PEPT2 which lacked the last three residues was not precipitated with PDZK1 (Figure 2b).

Furthermore, we demonstrated an association between endogenous PDZK1 and PEPT2 in human tissue by co-immunoprecipitating PEPT2 from human kidney membrane fractions using the anti-PDZK1 antibody, but not control immunoglobulin G (Figure 2c). This result is the evidence that observed interaction occurs between protein partners expressed from endogenous genes in kidneys.

Expression of PEPT2 in human kidney sections

In rats, Pept2 is present at the apical membrane of renal proximal tubules[14,15] and in humans, PDZK1 is reported to be expressed at the apical side of proximal tubular cells.[29,40] To determine whether PEPT2 and PDZK1 colocalize at the apical membrane of renal proximal tubules in humans, we carried out immunostaining of human serial kidney sections using anti-PEPT2 antibody.[41] Consistent with the previous reports, in the renal cortex, PEPT2 immunoreactivities were detected at the apical side of proximal tubular cells (Figure 3).

Table 1 | Characteristics of interaction between PEPT2 C-terminus and PDZK1 PDZ domains 2 and 3 (PDZ2 and PDZ3)

Construct	k_a (1/mM s)	k_d (1/min)	K_D (μM)
PDZK1-PDZ2	7.2×10^2	7.5×10^{-3}	10
PDZK1-PDZ3	3.6×10^2	5.5×10^{-3}	15

The kinetic characteristics of the interaction with immobilized GST-fused PEPT2 C-terminus with the second and third PDZ domains of PDZK1 (PDZ2 and PDZ3) fused with MBP measured by SPR methods are summarized. Association rate constants (k_a), dissociation rate constants (k_d), and equilibrium dissociation constants ($K_D = k_d/k_a$) are given.

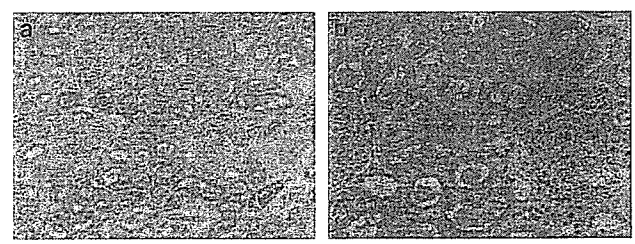

Figure 3 | Immunohistochemical analysis of PEPT2 in human kidney sections. (**a** and **b**) Immunohistochemical labeling of PEPT2 by diaminobenzidine reaction of human kidney. (**a**) PEPT2 was detected in proximal tubules in the cortex. (**b**) The apical membrane of proximal tubule was immunostained with the anti-hPET2 antibody and no immunostaining was observed in the basolateral membrane and glomeruli. These figures are representative of typical section samples. Original magnifications, (**a**) × 100 and (**b**) × 400.

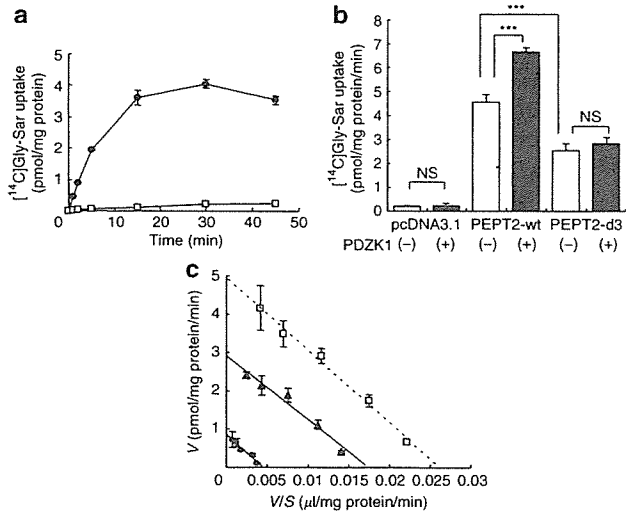

Figure 4 | Effect of PDZK1 on PEPT2-mediated [^{14}C]Gly-Sar transport activity. (**a**) The time profile of the uptake of [^{14}C]Gly-Sar via PEPT2. Intracellular accumulation of Gly-Sar was linear within 5 min and was significantly greater in PEPT2-wt-transfected HEK293 cells (HEK-PEPT2-wt; filled circles) than that in the mock-transfected cells (HEK-mock; open squares). (**b**) Coexpression of PEPT2 and PDZK1 increased [^{14}C]Gly-Sar uptake (30 μM) significantly over cells transfected with PEPT2 alone (closed column, middle). This effect was abolished when the C-terminal deletion mutant of PEPT2 was cotransfected with PDZK1 (HEK-PEPT2-d3; closed column, right), confirming that the interaction of PDZK1 with PEPT2 C-terminal domain is responsible for this effect. ***$P<0.001$ (**c**) Kinetic data using PEPT2-expressing HEK293 cells showed that PDZK1 (open squares) increased the V_{max} from 2.92 to 4.95 fmol/mg protein/min and increased the K_m slightly from 167 to 189 μM, as compared with PEPT2 alone (filled triangles). V_{max} of [^{14}C]Gly-Sar transport via HEK-PEPT2-d3 decreased (0.86 pmol/mg protein/min), whereas its K_m showed no change (187 nM) (filled circles). The kinetic parameters for the uptake via PEPT2 were estimated using $v = V_{max}[S]/(K_m + [S])$, where v is the uptake rate of substrates, $[S]$ is the substrate concentration (μM) in the medium. K_m is the Michaelis–Menten constant (μM) and V_{max} is the maximum uptake rate (pmol/mg of protein/2 min). These parameters were determined using the Eadie–Hofstee equation.

PEPT2 transport activity increases in presence of PDZK1

To determine whether PEPT2 and PDZK1 interaction is required to mediate the increase in PEPT2 transport activity, we transfected HEK293 cells with the pcDNA3.1(+) plasmid containing full-length PEPT2 (HEK-PEPT2-wt), PEPT2 lacking the last three amino acids (HEK-PEPT2-d3), or without an insert (HEK-mock). The time profile of the uptake of [^{14}C]glycylsarcosine (Gly-Sar) via PEPT2 is shown in Figure 4a. Intracellular accumulation of Gly-Sar was linear within 5 min and it was also significantly greater in HEK-PEPT2-wt than that in HEK-mock. After 2 min incubation, we demonstrated that [^{14}C]Gly-Sar uptake via HEK-PEPT2-wt was approximately 20-fold higher than that in HEK-mock and that in HEK-PEPT2-d3 was approximately 12-fold higher than that in HEK mock (Figure 4b). Gly-Sar transport activities significantly increased after PDZK1 coexpression (1.5-fold) (Figure 4b). This effect was not observed when PEPT2-d3 was coexpressed with PDZK1 (Figure 4b).

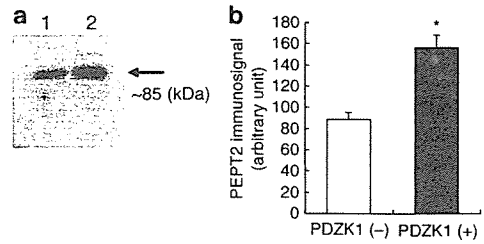

Figure 5 | Surface expression level of PEPT2. (**a**) cell surface biotinylation analysis of PEPT2 transiently expressing HEK293 cells transfected with vector alone (lane 1), and those transfected with PDZK1 (lane 2). Single bands of approximately 85 kDa, which are consistent with PEPT2, were observed in both lanes. (**b**) Quantification of immunosignal for PEPT2 ($n = 3$, error bars are s.d.). Densitometric analysis was performed using Model DIANA II Imaging System (M&S Instruments Trading Inc., Tokyo, Japan). *$P<0.05$.

Next, we examined the effect of PDZK1 coexpression on the kinetics of [^{14}C]Gly-Sar transport via HEK-PEPT2-wt that had been transfected with pcDNA3.1-PDZK1 or pcDNA3.1 alone. Kinetic data showed that PDZK1 significantly increased V_{max} from 2.92 to 4.95 pmol/mg protein/min and slightly increased K_m from 167 to 189 nM, in comparison to PEPT2 alone (Figure 4c). Interestingly, the V_{max} of [^{14}C]Gly-Sar transport via HEK-PEPT2-d3, decreased (0.86 pmol/mg protein/min), whereas its K_m showed no change (187 nM).

Surface expression level of PEPT2

To determine changes in the cell surface expression level of PEPT2, we used a cell-membrane-impermeant biotinylation reagent to selectively label the cell-surface proteins. After the treatment, the cell lysates from HEK293 cells transfected with PEPT2 and PDZK1 or PEPT2 and mock was collected. The amount of surface-biotinylated PEPT2 expression on plasma membranes increased 1.8-fold (PEPT2 and mock-transfected: 88.3 ± 6.9 vs PEPT2 and PDZK1-transfected: 155.5 ± 11.3 AU, $n = 3$) when PDZK1 was coexpressed (Figure 5). This change seems close to the one in V_{max} of PEPT2-mediated transport observed in Figure 4c.

DISCUSSION

The proton-coupled peptide transporter PEPT2 (*SLC15A2*) mediates the high-affinity low-capacity transport of small peptides in the kidney. Therefore, PEPT2 is presumed to contribute to the conservation of peptide-bound amino acids. Although the transport properties and characteristics of substrate recognition for PEPT2 have been well documented, there is less information on PEPT2 regulation. A recent report by Kato *et al.*[31] has provided the novel idea concerning the modulation of PEPT2 function by its associated protein. They demonstrated an interaction between the recombinant PEPT2 C-terminus fused to GST and purified His-tagged PDZK1, but they solely rely on data from *in vitro* binding assays and did not indicate the physiological importance of this interaction. In addition, the yeast two-hybrid screens performed by Gisler *et al.*,[42] using baits

containing single PDZ domains derived from mouse PDZK1, failed to detect Pept2 as a candidate for PDZK1 binding although several membrane proteins including Urat1 were found. To identify PDZK1 as a physiological binding partner of PEPT2, we evaluated this interaction from several viewpoints in this study.

Starting from a yeast two-hybrid screening of a human kidney cDNA library, we have demonstrated PDZK1 to be a physiological interactor of PEPT2. First, we could detect PDZK1 from 64 positive clones by library screening. Second, we could observe the co-immunoprecipitation of PEPT2 and PDZK1 from kidney membrane fractions (Figure 2c). Third, we could demonstrate the localization of PEPT2 protein at the apical side of the renal proximal tubules where PDZK1 is also expressed (Figure 3). These results indicate the physiological meaning of this interaction.

We have further examined this interaction by a yeast two-hybrid assay (Figure 1), an *in vitro* pull-down assay (Figure 2a), co-immunoprecipitation (Figure 2b) and surface plasmon resonance assay (Table 1) of recombinant proteins, as well as by the transport studies (Figure 4) and a cell surface biotinylation assay (Figure 5). These results support the preliminary data presented by Kato *et al.*[31] Moreover, the augmentation of the transport activity by PDZK1 was accompanied by a significant increase in the V_{max} of Gly-Sar transport via PEPT2 (Figure 4c) and was associated with the increased surface expression level of PEPT2 in HEK293 cells (Figure 5). These characteristics are closely similar to those of the URAT1–PDZK1 interaction,[29] and suggest PDZK1 to thus play a similar role in PEPT2–PDZK1 interaction; namely, that PEPT2 is stabilized and/or anchored at the cell membrane, making it less likely to be internalized and subsequently degraded.

Although their functional consequences are the same, there are several differences between the PEPT2–PDZK1 interaction and the URAT1–PDZK1 interaction. First, the frequency of PDZK1 appearing as a positive clones was smaller in the case of PEPT2 (one out of 64) than in the case of URAT1 (35 out of 98). Second, the interaction profiles of PDZK1 ligand against individual PDZ domains of PDZK1 were different, although they have similar C-terminal PDZ motifs: T-K-L for PEPT2 and T-Q-F for URAT1. PEPT2 binds to PDZ2 and PDZ3 (Figure 1), while URAT1 binds to PDZ1, PDZ2, and PDZ4.[29] Third, the binding affinities for each PDZ domain of PDZK1 were more than 10-fold lower for PEPT2 than for URAT1: 10 and 15 μM for PEPT2 (Table 1) and 1.97–514 nM for URAT1.[29] Fourth, when a C-terminal deletion mutant of URAT1 (URAT1-d3) was coexpressed with PDZK1, urate transport activity was not enhanced, but URAT1-d3 still demonstrated a similar urate transport activity to wt URAT1 when expressed without PDZK1. In contrast, the C-terminal deletion mutant of PEPT2 (PEPT2-d3) not only lacked the ability to enhance transport activity when coexpressed with PDZK1, but its transport activity was reduced to half that of the wt PEPT2 (PEPT2-wt) when expressed without PDZK1.

The low frequency of PDZK1 in PEPT2 screening seems consistent with the report of Gisler *et al.*[42] as we mentioned earlier in this paper. In addition to the expression levels of these proteins, the binding affinity is likely to affect the frequency of a particular protein appearing as a positive clone in yeast two-hybrid screening. Therefore, a low frequency of positive clone does not mean that the observed interaction is physiologically less important. Moreover, a low binding affinity may be advantageous for the regulatory dynamics of protein–protein interactions,[27] because a low binding affinity is related to an easier association and dissociation of proteins than a high binding affinity. In particular, PEPT2 has a putative protein kinase C (PKC) recognition site at its C-terminal close to the PDZ motif, whose phosphorylation may interfere with binding to the PDZ domain.[43] It will be interesting to investigate whether the phosphorylation of both PEPT2 and PDZK1 or either protein independently alters the binding affinity of this interaction, in order to clarify the regulatory mechanism for PDZ–ligand interaction.

The decreased transport activity of the PEPT2 C-terminal deletion mutant compared to wt PEPT2, together with the significant reduction in V_{max} (Figure 4) may indicate PDZ motif to thus play another role in the PEPT2-CT: the targeting of the transporter to the plasma membrane. This was originally predicted by Russel *et al.*[28] However, as mentioned above, this phenomenon was not observed in the C-terminal deletion mutant of URAT1 expressed in the same HEK293 cells that have endogenous PDZK1 at low level.[29] Although we frequently detected PDZK1 in the URAT1 screen, we did not find any other binding candidates for URAT1. In the PEPT2 screen, we detected several potential binding partners for PEPT2 besides PDZK1 (manuscript in preparation). It will therefore be important to identify other binding proteins surrounding PEPT2 to understand the potential significance of this interaction.

Recently, PDZ proteins have been recognized as orchestrating scaffolds to achieve concerted functions.[23] PEPT2 mediates an electrogenic proton-coupled cotransport that uses an inward proton gradient to transport small peptides from urine to the cell. Following the concept proposed by Moe, the ability of PDZK1 to couple PEPT2 to the Na^+/H^+ exchanger NHE3 may provide the necessary lumen-to-cell proton gradient, and the multimolecular protein complex will be functionally equivalent to a Na^+/oligopeptide cotransporter. A functional coupling between PEPT2 and NHE1 and/or NHE2 has recently been shown by Wada *et al.*[44] In this paper, we described, for the first time, the exact localization of PEPT2 in the human kidney in addition to its novel regulatory mechanism. PEPT2 proteins are expressed at the apical membrane of renal proximal tubules similarly to rat Pept1 and rat Pept2, which are expressed in the same site.[15] Based on the above findings, human PEPT2 may therefore be involved in the reabsorption of peptides on the apical side of the renal tubules, similar to that of rodent Pept2 and the protein complex surrounding PEPT2 should thus be clarified by identifying other interacting proteins to obtain a

Table 2 | PCR primers used in this study

Construct	Sense primer	Antisense primer
PEPT2-CTwt	5′-CGAATTCCTGCCCGAGACCCAGAG-3′	5′-CTCTCGAGCTAAAACTGTGTGGATTTTA-3′
PEPT2-CTd3	5′-CGAATTCCTGCCCGAGACCCAGAG-3′	5′-CCCTCGAGCTAGGATTTTAGGACAGAGTTC-3′
PEPT2-L727A	5′-CGAATTCCTGCCCGAGACCCAGAG-3′	5′-CCCTCGAGCTAAGCCTGTGTGGATTTTAGGA-3′
PEPT2-T729A	5′-CGAATTCCTGCCCGAGACCCAGAG-3′	5′-CCCTCGAGCTAAAACTGTGCGGATTTTA-3′

PCR, polymerase chain reaction; wt, wild type.

comprehensive understanding of the peptide transport function in the renal proximal tubules.

MATERIALS AND METHODS

Materials

[^{14}C]Glycosylsarcosine (Gly-Sar) (4 Ci/mmol) was obtained from Moravek (Brea, CA, USA). Other materials used included Ham F12 medium from Nissui Pharmaceutical Co., Ltd. (Tokyo, Japan), and fetal bovine serum and trypsin from Invitrogen (Carlsbad, CA, USA).

Cloning of human PEPT2 cDNA

The cDNA library was prepared from human kidney poly(-A)$^+$RNA.[45] The 0.46-kb cDNA fragment (24–481 nt of the nucleotide sequence of human PEPT2 (hPEPT2)) was obtained by polymerase chain reaction. This fragment was labeled with [^{32}P]dCTP (T7QuickPrime, Amersham Biosciences, Tokyo, Japan) and used as probe. The screening of the cDNA library was performed as described elsewhere.[46]

Plasmid construction

The C-terminal fragments of wt hPEPT2 cDNA and three mutants (designated d3, L729A, and T727A) were generated by polymerase chain reaction using specific primers (Table 2) and cloned into the *Bam*HI and *Xho*I sites of pEG202 (bait) and pGEX-6P-1 (Amersham Biosciences) to construct PEPT2-CTwt, PEPT2-CTd3, PEPT2-L729A, and PEPT2-T727A. The full-length coding sequences of hPEPT2 (wt) as well as its C-terminal 3-amino-acid-deletion mutant (d3) were inserted into the mammalian expression vector pcDNA3.1 (Invitrogen) for functional analysis and into pEGFP-C2 (Clontech, Tokyo, Japan) for GFP fusion protein preparation. The pcDNA3.1 vector containing the full-length human PDZK1 (hPDZK1) and preys (pJG4–5 and pMAL-C2x) containing single PDZ domains of hPDZK1 were prepared as described previously.[29]

Yeast two-hybrid assay

A human kidney cDNA library was constructed as described previously.[29] A PEPT2 C-terminal bait corresponding to the last 34 amino acids of PEPT2 was used to screen 8.7×10^6 clones of the human kidney cDNA library with the LexA-based GFP two-hybrid system (Grow'n' Glow system; MoBiTec, Göttingen, Germany).

In vitro binding assay

PEPT2-CT for GST fusion protein production in bacteria as reported previously.[47] *In vitro* translation was performed from a plasmid carrying the full-length PDZK1 with the TNT T7 Quick for polymerase chain reaction DNA system (Promega, Tokyo, Japan) in the presence of Transcend Biotinylated tRNA (Promega), as described elsewhere.[29] Of *in vitro*-translated products, (5 μl) was applied into ProFound™ Pull-Down GST Protein:Protein Interaction Kit (Pierce, Rockford, IL, USA) with 50 μl of GST-glutathione-Sepharose resin and protein complexes were eluted according to the manufacturer's instructions.

Surface plasmon resonance

The interactions of PEPT2-CT with the second and third PDZ domains of PDZK1 were investigated using a BIAcore 3000 analytical system (BIAcore AB, Tokyo, Japan). Using an amine coupling kit, GST-fused wt PEPT2-CT or GST alone was attached to a CM5 sensor chip according to the manufacturer's instructions, giving an increase of 11 214 resonance units (RU) for GST-PEPT2-CT or 8,566 resonance units for GST alone. Binding experiments were performed with the PDZK1 single PDZ domains fused with maltose-binding protein as described elsewhere.[29]

Immunohistochemical analysis

We used human single-tissue slides (Biochain, Hayward, CA, USA) for light microscopic immunohistochemical analysis as reported previously.[48] They were treated with 10 μg/ml primary rabbit polyclonal antibodies against PEPT2[41] or PDZK1 (4°C overnight).

Cell culture and transfection

HEK293 cells were maintained in Dulbecco's-modified Eagle's medium supplemented with 10% fetal bovine serum, 1 mM sodium pyruvate, penicillin (100 U/ml), and streptomycin (100 mg/ml) (Invitrogen) at 37°C in 5% CO_2. Transient transfection with Lipofectamine 2000 (Invitrogen, Gaithersburg, MD, USA) was performed according to the manufacturer's recommendations.

Immunoprecipitation and immunoblotting

Immunoprecipitation analysis was performed as described previously.[49] Lysates from HEK293 cells that expressed GFP-fused hPEPT2 and hPDZK1 were immunoprecipitated by the anti-GFP antibody (full-length A.v. polyclonal antibody, Clontech). For the co-immunoprecipitation of endogenous PEPT2 and PDZK1, we used human kidney membrane fractions (Biochain) and added the anti-PEPT2 antibody or control immunoglobulin G to this solution. After overnight incubation, PEPT2 and PDZK1 were immunoprecipitated using the Seize Classic (A) Immunoprecipitation kit (Pierce). The affinity-purified rabbit PDZK1 antibody and horseradish peroxidase-conjugated goat anti-rabbit immunoglobulin G (Amersham Biosciences) were used for immunoblotting with enhanced chemiluminescence reagents (ECL Plus, Amersham Biosciences).

Gly-Sar transport activity assay

HEK293 cells were plated on 24-well culture plates at a density of 2×10^5 cells/well 24 h prior to transfection, and they were transfected as described above. After 36 h, the culture medium was removed, and the cells were washed three times and incubated in

serum-free Hank's solution (containing in mM: 125 NaCl, 5.6 glucose, 4.8 KCl, 1. 2 $MgSO_4 \cdot 7H_2O$, 1.2 KH_2PO_4, 1.3 $CaCl_2 \cdot 2H_2O$, 25 *N*-2-hydroxyethylpiperazine-*N'*-2-ethanesulfonic acid (pH 6.0)) for 10 min. The uptake study was started by adding 500 μl of solution containing 30 μM [^{14}C]Gly-Sar to the plate. After 2 min, the cells were washed twice in an ice-cold solution, and lysed in 0.1 N NaOH for 20 min for scintillation counting.

To determine the kinetic parameters, the concentrations of Gly-Sar were varied from 30 to 1000 μM. PEPT2-mediated Gly-Sar uptake was calculated as the difference between the uptake rates into HEK293 cells transiently expressing PEPT2 and those into HEK293 cells transfected with the vector (pcDNA3.1, Invitrogen) only.

Cell surface biotinylation

Surface biotinylation of PEPT2 at the plasma membrane was performed as described elsewhere.[49] Surface proteins in HEK293 cells transfected with pcDNA3.1(+)-hPEPT2 and pcDNA3.1(+)-hPDZK1 or pcDNA3.1(+) empty vector (mock) were biotinylated with Sulfo-NHS-SS-Biotin (Pierce) (0.5 mg/ml) in phosphate-buffered saline for 30 min at 4°C. Cell lysates were then incubated with Ultralink-immobilized NeutrAvidin beads (Pierce) to precipitate biotinylated proteins. PEPT2 was detected with polyclonal PEPT2 antibody (1:10,000).[41]

Statistical analysis

Uptake experiments were conducted three times, and each uptake experiment was performed in triplicate. Values are presented as the mean $\pm$ s.e. Statistical significance was determined by Student's *t*-test.

ACKNOWLEDGMENTS

We thank Akie Toki and Keiko Sakama for technical assistance. The anti-hPDZK1 polyclonal antibody was supplied by Transgenic Inc., Kumamoto, Japan. This work was supported in part by grants from the Ministry of Education, Culture, Sports, Science and Technology of Japan, the Japan Society for the Promotion of Science, Research on Health Sciences focusing on Drug Innovation from the Japan Health Sciences Foundation, Mutual Aid Corporation for Private Schools of Japan, the Nakatomi Foundation, the Salt Science Research Foundation (No. 0524), the Japan Foundation of Applied Enzymology, Astellas Foundation for Research on Metabolic Disorders, Gout Research Foundation of Japan, Heiwa Nakajima Foundation, and Health and Labor Sciences Research Grants for Research on Advanced Medical Technology: Toxicogenomics Project. This work was presented in part at the Annual Meeting of Experimental Biology 2004, Washington DC, April 2004, and published in abstract form (*FASEB J* **18**:A695, 2004).

REFERENCES

1. Daniel H, Rubio-Aliaga I. An update on renal peptide transporters. *Am J Physiol Renal Physiol* 2003; **284**: F885–F892.
2. Nielsen CU, Brodin B. Di/tri-peptide transporters as drug delivery targets: regulation of transport under physiological and patho-physiological conditions. *Curr Drug Targets* 2003; **4**: 373–388.
3. Terada T, Inui K. Peptide transporters: structure, function, regulation and application for drug delivery. *Curr Drug Metab* 2004; **5**: 85–94.
4. Boll M, Markovich D, Weber WM *et al.* Expression cloning of a cDNA from rabbit small intestine related to proton-coupled transport of peptides, lactam antibiotics and ACE-inhibitors. *Pflugers Arch* 1994; **429**: 146–149.
5. Fei YJ, Kanai Y, Nussberger S *et al.* Expression cloning of a mammalian proton-coupled oligopeptide transporter. *Nature* 1994; **368**: 563–566.
6. Boll M, Herget M, Wagener M *et al.* Expression cloning and functional characterization of the kidney cortex high-affinity proton-coupled peptide transporter. *Proc Natl Acad Sci USA* 1996; **93**: 284–289.
7. Saito H, Okuda M, Terada T *et al.* Cloning and characterization of a rat H+/peptide cotransporter mediating absorption of β-lactam antibiotics in the intestine and kidney. *J Pharmacol Exp Ther* 1995; **275**: 1631–1637.
8. Miyamoto KI, Shiraga T, Morita K *et al.* Sequence, tissue distribution and developmental changes in rat intestinal oligopeptide transporter. *Biochim Biophys Acta* 1996; **1305**: 34–38.
9. Saito H, Terada T, Okuda M *et al.* Molecular cloning and tissue distribution of rat peptide transporter PEPT2. *Biochim Biophys Acta* 1996; **1280**: 173–177.
10. Liang R, Fei YJ, Prasad PD *et al.* Human intestinal H^+/peptide cotransporter. Cloning, functional expression, and chromosomal localization. *J Biol Chem* 1995; **270**: 6456–6463.
11. Liu W, Liang R, Ramamoorthy S *et al.* Molecular cloning of PEPT2, a new member of the H^+/peptide cotransporter family, from human kidney. *Biochim Biophys Acta* 1995; **1235**: 461–466.
12. Ramamoorthy S, Liu W, Ma YY *et al.* Proton/peptide cotransporter (PEPT2) from human kidney: functional characterization and chromosomal localization. *Biochim Biophys Acta* 1995; **1240**: 1–4.
13. Smith DE, Pavlova A, Berger UV *et al.* Tubular localization and tissue distribution of peptide transporters in rat kidney. *Pharm Res* 1998; **15**: 1244–1249.
14. Ogihara H, Saito H, Shin BC *et al.* Immuno-localization of H^+/peptide cotransporter in rat digestive tract. *Biochem Biophys Res Commun* 1996; **220**: 848–852.
15. Shen H, Smith DE, Yang T *et al.* Localization of PEPT1 and PEPT2 proton-coupled oligopeptide transporter mRNA and protein in rat kidney. *Am J Physiol* 1999; **276**: F658–F665.
16. Rubio-Aliaga I, Frey I, Boll M *et al.* Targeted disruption of the peptide transporter Pept2 gene in mice defines its physiological role in the kidney. *Mol Cell Biol* 2003; **23**: 3247–3252.
17. Takahashi K, Masuda S, Nakamura N *et al.* Upregulation of H(+)-peptide cotransporter PEPT2 in rat remnant kidney. *Am J Physiol Renal Physiol* 2001; **281**: F1109–F1116.
18. Nakamura N, Masuda S, Takahashi K *et al.* Decreased expression of glucose and peptide transporters in rat remnant kidney. *Drug Metab Pharmacokinet* 2004; **19**: 41–47.
19. Wenzel U, Diehl D, Herget M *et al.* Regulation of the high-affinity H+/peptide cotransporter in renal LLC-PK1 cells. *J Cell Physiol* 1999; **178**: 341–348.
20. Bravo SA, Nielsen CU, Amstrup J *et al.* Epidermal growth factor decreases PEPT2 transport capacity and expression in the rat kidney proximal tubule cell line SKPT0193 cl.2. *Am J Physiol Renal Physiol* 2004; **286**: F385–F393.
21. Biber J. Emerging roles of transporter-PDZ complexes in renal proximal tubular reabsorption. *Pflugers Arch* 2001; **443**: 3–5.
22. Levi M. Role of PDZ domain-containing proteins and ERM proteins in regulation of renal function and dysfunction. *J Am Soc Nephrol* 2003; **14**: 1949–1951.
23. Moe OW. Scaffolds: orchestrating proteins to achieve concerted function. *Kidney Int* 2003; **64**: 1916–1917.
24. Anzai N, Jutabha P, Kanai Y, Endou H. Integrated physiology of proximal tubular organic anion transport. *Curr Opin Nephrol Hypertens* 2005; **14**: 472–479.
25. Fanning AS, Anderson JM. Protein modules as organizers of membrane structure. *Curr Opin Cell Biol* 1999; **11**: 432–439.
26. Garner CC, Nash J, Huganir RL. PDZ domains in synapse assembly and signalling. *Trends Cell Biol* 2000; **10**: 274–280.
27. Hung AY, Sheng M. PDZ domains: structural modules for protein complex assembly. *J Biol Chem* 2002; **277**: 5699–5702.
28. Russel FGM, Masereeuw R, van Aubel RAMH. Molecular aspects of renal anionic drug transport. *Annu Rev Physiol* 2002; **64**: 563–594.
29. Anzai N, Miyazaki H, Noshiro R *et al.* The multivalent PDZ domain-containing protein PDZK1 regulates transport activity of renal urate-anion exchanger URAT1 via its C-terminal. *J Biol Chem* 2004; **279**: 45942–45950.
30. Anzai N, Enomoto A, Endou H. Renal urate handling: clinical relevance of recent advances. *Curr Rheumatol Rep* 2005; **7**: 227–234.
31. Kato Y, Yoshida K, Watanabe C *et al.* Screening of the interaction between xenobiotic transporters and PDZ proteins. *Pharm Res* 2004; **21**: 1886–1894.
32. Kocher O, Comella N, Tognazzi K, Brown LF. Identification and partial characterization of PDZK1: a novel protein containing PDZ interaction domains. *Lab Invest* 1998; **78**: 117–125.
33. Hernando N, Wagner CA, Gisler SM *et al.* PDZ proteins and proximal ion transport. *Curr Opin Nephrol Hypertens* 2004; **13**: 569–574.

34. Weinman EJ, Steplock D, Wang Y, Shenolikar S. Characterization of a protein cofactor that mediates protein kinase A regulation of the renal brush border membrane Na^+-H^+ exchanger. *J Clin Invest* 1995; **95**: 2143–2149.
35. Reczek D, Berryman M, Bretscher J. Identification of EBP50: a PDZ-containing phosphoprotein that associates with members of the ezrin-radixin-moesin family. *J Cell Biol* 1997; **139**: 169–179.
36. Hall RA, Ostedgaard LS, Premont RT *et al.* A C-terminal motif found in the beta2-adrenergic receptor, P2Y1 receptor and cystic fibrosis transmembrane conductance regulator determines binding to the Na^+/H^+ exchanger regulatory factor family of PDZ proteins. *Proc Natl Acad Sci USA* 1998; **95**: 8496–8501.
37. Scott RO, Thelin WR, Milgram SL. A novel PDZ protein regulates the activity of guanylyl cyclase C, the heat-stable enterotoxin receptor. *J Biol Chem* 2002; **277**: 22934–22941.
38. Songyang Z, Fanning AS, Fu C *et al.* Recognition of unique carboxyl-terminal motifs by distinct PDZ domains. *Science* 1997; **275**: 73–77.
39. Harris BZ, Lim WA. Mechanism and role of PDZ domains in signaling complex assembly. *J Cell Sci* 2001; **114**: 3219–3231.
40. Kocher O, Comella N, Gilchrist A *et al.* PDZK1, a novel PDZ domain-containing protein up-regulated in carcinomas and mapped to chromosome 1q21, interacts with cMOAT (MRP2), the multidrug resistance-associated protein. *Lab Invest* 1999; **79**: 1161–1170.
41. Terada T, Irie M, Okuda M, Inui K. Genetic variant Arg57His in human H^+/peptide cotransporter 2 causes a complete loss of transport function. *Biochem Biophys Res Commun* 2004; **316**: 416–420.
42. Gisler SM, Pribanic S, Bacic D *et al.* PDZK1: I. A major scaffolder in brush borders of proximal tubular cells. *Kidney Int* 2003; **64**: 1733–1745.
43. Daniel H, Herget M. Cellular and molecular mechanisms of renal peptide transport. *Am J Physiol* 1997; **273**: F1–F8.
44. Wada M, Miyakawa S, Shimada A *et al.* Functional linkage of H^+/peptide transporter PEPT2 and Na^+/H^+ exchanger in primary cultures of astrocytes from mouse cerebral cortex. *Brain Res* 2005; **1044**: 33–41.
45. Cha SH, Sekine T, Fukushima J *et al.* Identification and characterization of human organic anion transporter 3 expressing predominantly in the kidney. *Mol Pharmacol* 2001; **59**: 1277–1286.
46. Sakata T, Anzai N, Shin HJ *et al.* Novel single nucleotide polymorphisms of organic cation transporter 1 (*SLC22A1*) affecting transport functions. *Biochem Biophys Res Commun* 2004; **313**: 789–793.
47. Anzai N, Deval E, Schaefer L *et al.* The multivalent PDZ domain-containing protein CIPP is a partner of acid-sensing ion channel 3 in sensory neurons. *J Biol Chem* 2002; **277**: 16655–16661.
48. Ekaratanawong S, Anzai N, Jutabha P *et al.* Human organic anion transporter 4 is a renal apical organic anion/dicarboxylate exchanger in the proximal tubules. *J Pharmacol Sci* 2004; **94**: 297–304.
49. Miyazaki H, Anzai N, Ekaratanawong S *et al.* Modulation of renal apical organic anion transporter 4 (OAT4) function by two PDZ domain-containing proteins. *J Am Soc Nephrol* 2005; **16**: 3498–3506.

Identification and Functional Characterization of a New Human Kidney–Specific H^+/Organic Cation Antiporter, Kidney-Specific Multidrug and Toxin Extrusion 2

Satohiro Masuda,* Tomohiro Terada,* Atsushi Yonezawa,* Yuko Tanihara,* Koshiro Kishimoto,* Toshiya Katsura,* Osamu Ogawa,† and Ken-ichi Inui*

**Department of Pharmacy, Kyoto University Hospital, Faculty of Medicine, and †Department of Urology, Graduate School of Medicine, Kyoto University, Kyoto, Japan*

A cDNA coding a new H^+/organic cation antiporter, human kidney-specific multidrug and toxin extrusion 2 (hMATE2-K), has been isolated from the human kidney. The hMATE2-K cDNA had an open reading frame that encodes a 566–amino acid protein, which shows 94, 82, 52, and 52% identity with the hMATE2, hMATE2-B, hMATE1, and rat MATE1, respectively. Reverse transcriptase–PCR revealed that hMATE2-K mRNA but not hMATE2 was expressed predominantly in the kidney, and hMATE2-B was ubiquitously found in all tissues examined except the kidney. The immunohistochemical analyses revealed that the hMATE2-K as well as the hMATE1 was localized at the brush border membranes of the proximal tubules. HEK293 cells that were transiently transfected with the hMATE2-K cDNA but not hMATE2-B exhibited the H^+ gradient–dependent antiport of tetraethylammonium (TEA). Transfection of hMATE2-B had no affect on the hMATE2-K–mediated transport of TEA. hMATE2-K also transported cimetidine, 1-methyl-4-phenylpyridinium (MPP), procainamide, metformin, and N^1-methylnicotinamide. Kinetic analyses demonstrated that the Michaelis-Menten constants for the hMATE2-K–mediated transport of TEA, MPP, cimetidine, metformin, and procainamide were 0.83 mM, 93.5 μM, 0.37 mM, 1.05 mM, and 4.10 mM, respectively. Ammonium chloride–induced intracellular acidification significantly stimulated the hMATE2-K–dependent transport of organic cations such as TEA, MPP, procainamide, metformin, N^1-methylnicotinamide, creatinine, guanidine, quinidine, quinine, thiamine, and verapamil. These results indicate that hMATE2-K is a new human kidney–specific H^+/organic cation antiporter that is responsible for the tubular secretion of cationic drugs across the brush border membranes.

J Am Soc Nephrol 17: 2127–2135, 2006. doi: 10.1681/ASN.2006030205

Vectorial secretion of cationic compounds across the tubular epithelial cells is an important function of the kidney. Using the stopped flow tubular microperfusion method, cultured renal epithelial cells, and isolated membrane vesicles, it was suggested that two functionally distinct organic cation transporters were expressed in the basolateral and brush border membranes, respectively (1,2). Organic cations are suggested to accumulate in the renal tubular cells *via* a basolateral organic cation transport system that is sensitive to membrane potential differences. The intracellular cationic compounds were secreted by the apical H^+/organic cation antiport system, which was driven by an oppositely directed H^+ gradient. A prototype substrate, tetraethylammonium (TEA), has been used consistently for the functional characterization of these organic cation transport systems in the kidney (3–7).

Since cloning of the organic cation transporter OCT1 from the rat kidney (8), many related transporter proteins have been cloned and characterized. It is widely known that the basolateral entry of cationic compounds is mediated mainly by hepatic hOCT1 (SLC22A1) and renal hOCT2 (SLC22A2) in humans, depending on the membrane potential (9–11). However, attempts at molecular identification of the apical H^+/organic cation antiporter have failed for more than a decade. Recently, *in silico* homology screening of the human cDNA database identified a H^+/organic cation antiporter, human multidrug and toxin extrusion 1 (hMATE1), from the human brain using the NorM Na^+/multidrug antiporter in *Vibrio parahaemolyticus* as a reference (12). hMATE1 was expressed in the liver, kidney, and skeletal muscle and weakly in the brain and the heart. Although an isoform of hMATE1, hMATE2, was reported simultaneously to be expressed primarily in the kidney, the functional characteristics of hMATE2 were not examined.

In this study, we cloned hMATE2 cDNA from the human kidney for functional characterization. Sequence analysis revealed that the newly cloned cDNA was an alternative splice variant of hMATE2. It is interesting that real-time PCR and reverse transcriptase–PCR (RT-PCR) analyses clearly indicated that the newly cloned hMATE2 but not the original hMATE2 was expressed only in the kidney, showing a function of oppositely directed H^+ gradient–dependent antiport of organic

Received March 7, 2006. Accepted May 15, 2006.

Published online ahead of print. Publication date available at www.jasn.org.

Address correspondence to: Prof. Ken-ichi Inui, Department of Pharmacy, Kyoto University Hospital, Faculty of Medicine, Kyoto University, Sakyo-ku, Kyoto 606-8507, Japan. Phone: +81-75-751-3577; Fax: +81-75-751-4207; E-mail: inui@kuhp.kyoto-u.ac.jp

ISSN: 1046-6673/1708-2127

cations; therefore, we designated the new clone human kidney-specific multidrug and toxin extrusion (hMATE2-K).

Materials and Methods

[^{14}C]TEA (2.035 GBq/mmol), [^{14}C]creatinine (2.035 GBq/mmol), [^{14}C]procainamide (2.035 GBq/mmol), [methyl-^{14}C]choline (2.035 GBq/mmol), [9-^{3}H]quinidine (740 GBq/mmol), [^{3}H]quinine (740 GBq/mmol), [^{3}H (G)]thiamine (370 GBq/mmol), L-[N-methyl-^{3}H]carnitine (3.145 TBq/mmol), [N-methyl-^{14}C]nicotine (2.035 TBq/mmol), [N-methyl-^{3}H]verapamil (2.96 TBq/mmol), and [7-^{3}H (N)]tetracycline (185 GBq/mmol) were obtained from American Radiolabeled Chemicals Inc. (St. Louis, MO). [^{14}C]Metformin (962 MBq/mmol) and [^{14}C]guanidine hydrochloride (1.961 GBq/mmol) were purchased from Moravek Biochemicals Inc. (Brea, CA). [^{3}H]1-Methyl-4-phenylpyridinium acetate (MPP; 2.7 TBq/mmol), [^{14}C]*p*-aminohippuric acid (1.9 GBq/mmol), and [^{3}H]glycylsarcosine (148 GBq/mmol) were from PerkinElmer Life Analytical Sciences (Boston, MA). [*N*-Methyl-^{3}H]Cimetidine (451 GBq/mmol) was from Amersham Biosciences (Uppsala, Sweden). [^{14}C]Levofloxacin (1.07 GBq/mmol) was from Daiichi Pharmaceutical Co., Ltd. (Tokyo, Japan). N^{1}-Methylnicotinamide (NMN) was obtained from Sigma (St. Louis, MO). [^{14}C]Captopril (0.115 GBq/mmol; Sankyo Co., Tokyo, Japan), cephalexin (Shionogi, Osaka, Japan), cefazolin (Astellas Pharma Inc., Tokyo, Japan), and cephradine (Sankyo Co.) were gifts from the respective suppliers. All other chemicals used were of the highest purity available.

Isolation of hMATE2-K cDNA

The hMATE2 cDNA was cloned by RT-PCR from Marathon-Ready human kidney cDNA (Clontech, Palo Alto, CA). Primers that are specific for hMATE2 were designed on the basis of the sequence information of FLJ31196 (NM_152908). The forward and reverse primers, with mutations creating restriction enzyme sites (italics) for cloning the hMATE2 cDNA, were 5′-AGGGTACCCAGTGCCCCGGCCAGGAATGGA-3′ and 5′-CTGTC*TAGACCCCTCTGAGTGTCACCACAA*-3′, respectively. Simultaneously, hMATE2 cDNA was cloned using the Marathon-Ready human brain cDNA (Clontech) as above. The PCR product was subcloned into the expression vector pcDNA3.1 (+) (Invitrogen, Carlsbad, CA) and sequenced using a multicapillary DNA sequencer RISA384 system (Shimadzu, Kyoto, Japan). Because both hMATE2 from the human kidney and brain were suggested to be splice variants of hMATE2 (FLJ31196) (12), we redesignated newly isolated clones from the human kidney and the human brain as hMATE2-K and hMATE2-B, respectively (Figure 1). The nucleotide sequences of hMATE2-K and hMATE2-B have been submitted to the DDBJ/EMBL/GenBank Data Bank as accession nos. AB250364 and AB250701, respectively.

Real-Time PCR and RT-PCR

Total RNA from various human tissues was purchased from BioChain (Hayward, CA). RT of the total RNA (500 ng/20 μl reaction) and real-time PCR were carried out as described previously (13). The primer-probe sets used for hMATE1 and hMATE2 are summarized in Table 1. Glyceraldehyde-3-phosphate dehydrogenase (GAPDH) mRNA was checked for the quality of the total RNA of human tissues used with GAPDH Control Reagent (Applied Biosystems). To detect independently both hMATE2-K and hMATE2 mRNA, we designed qualitative PCR primers as summarized in Table 1.

Polyclonal Antibodies and Immunohistochemical Analyses

Polyclonal antibodies were raised against the synthetic peptide that corresponded to the intracellular domains of hMATE1 (CQQAQVHANLKVN, no. 466-478) or hMATE2-K (YSRSECHVDFFRTPEE, no. 543-558) as described, respectively (14,15). For immunofluorescence histochemistry, the human renal specimens were fixed with 4% paraformaldehyde in PBS at 4°C for 30 min (13). Fixed tissues were embedded in OCT compound (Sakura Finetechnical, Tokyo, Japan) and frozen rapidly in liquid nitrogen. Sections (6 μm thick) were cut and covered with 2% FBS and 1 mg/ml RNase A (Nacalai Tesque, Kyoto, Japan) for 1 h. The covered sections were incubated for 1 h with antiserum (1:100 dilution) specific for hMATE1, hMATE2-K, hOCT2, a control of basolateral transporter, or hOCTN2, a control of luminal transporter, and then incubated with Cy3-labeled donkey anti-rabbit IgG (CALTAG Laboratory, San Francisco, CA), 5 U/ml Alexa 488-phalloidin (Molecular Probe, Eugene, OR), and 4′,6-diamidino-2-phenylindole for 1 h. These sections were examined with a BX-50-FLA fluorescence microscope (Olympus, Tokyo, Japan) at ×100 magnification. Images were captured with a DP-50 CCD camera (Olympus) using Studio Lite software (Olympus). As controls, specific rabbit antibodies were replaced with preimmune rabbit serum.

```
hMATE2-K  532 ------------------------------------------------------------ 532
hMATE2-B  532 GCAGGTGAGAGGCTGTGCGTCCCAGCCTCTTCCAACTCCTCAACAGGGATGGCTGAAGGG 591
hMATE2    532 ----------------------------------------GGATGGCTGAAGGG 545

hMATE2-K  532 ------------------------------------------------------------ 532
hMATE2-B  592 GCAGGAGGAGGAGTCCCCATTCCAAACCCCGGGTTTGTCCATCCTCCATCCATCTCACTC 651
hMATE2    546 GCAGGAGGAGGAGTCCCCATTCCAAACCCCGGGTTTGTCCATCCTCCATCCATCTCACTC 605

hMATE2-K  532 ----------------------------------AAGATCACCTGGCCCCAAGTCCTCAG 557
hMATE2-B  652 ACACCTTAGCAGGGCCAGTTTTCATTTATTTCAG..... 711
hMATE2    606 ACACCTTAGCAGGGCCAGTTTTCATTTATTTCAG..... 665

hMATE2-K  558 TGGTGTGGTGGGCAACTGTGTCAACGGTGTGGCCAACTATGCCCTGGTTTCTGTGCTGAA 617
hMATE2-B  712 ..... 771
hMATE2    666 ..... 725

hMATE2-K  618 CCTGGGGGTCAG 629
hMATE2-B  772 ..... 783
hMATE2    726 ..... 737
```

Figure 1. Comparison of the nucleotide sequences of the exon 7 region among human kidney-specific multidrug and toxin extrusion 2 (hMATE2-K), human brain-specific multidrug and toxin extrusion 2 (hMATE2-B), and human multidrug and toxin extrusion 2 (hMATE2). Conserved nucleotides among three transporters are indicated by dots. The nucleotides are numbered starting at the first residue of the ATG putative initiation codon.

Cell Culture, Transfection, and Uptake Experiments

HEK293 cells (American Type Culture Collection CRL-1573, Manassas, VA) were cultured as described previously (16,17). pcDNA3.1 (+) plasmid vector DNA that contained hMATE2-K cDNA and hMATE2-B cDNA were transfected into HEK293 cells using LipofectAMINE 2000 Reagent (Invitrogen), as described (16,17). At 48 h after the transfection, the cells were used for uptake experiments.

Cellular uptake of cationic compounds was measured with monolayer cultures of HEK293 cells that were grown on poly-D-lysine–coated 24-well plates (16,17). Typically, the cells were preincubated with 0.2 ml of incubation medium (pH 7.4) for 10 min at 37°C. The medium then was removed, and 0.2 ml of incubation medium that contained radiolabeled substrates was added. The medium was aspirated off at the end of the incubation, and the monolayers were rinsed rapidly twice with 1 ml of ice-cold incubation medium. The cells were solubilized in 0.5 ml of 0.5 N NaOH, and then the radioactivity in aliquots was determined by liquid scintillation counting. The cellular uptake of cephalexin, cefazolin, and cephradine was described previously (18). For the cellular uptake of NMN, the HEK293 cells that were transfected with the hMATE2-K cDNA were incubated with NMN for 10 min, washed twice, and scraped with 0.5 ml of incubation medium (pH 7.4). The cellular accumulation of NMN was determined by HPLC